Epitaxial growth, magnetic properties, and lattice dynamics of Fe nanoclusters on GaAs(001)

B. Roldan Cuenya* and A. Naitabdi
Physics Department, University of Central Florida, Orlando, Florida 32816-2385, USA

E. Schuster, R. Peters, M. Doi,† and W. Keune
Fachbereich Physik, Universität Duisburg-Essen (Campus Duisburg), D-47048 Duisburg, Germany
(Received 13 September 2005; revised manuscript received 3 May 2007; published 10 September 2007)

Epitaxial bcc-Fe(001) ultrathin films have been grown at ~50 °C on reconstructed GaAs(001)-(4×6) surfaces and investigated *in situ* in ultrahigh vacuum (UHV) by reflection high-energy electron diffraction, scanning tunneling microscopy (STM), x-ray photoelectron spectroscopy (XPS), and ^{57}Fe conversion electron Mössbauer spectroscopy (CEMS). For t_{Fe}=1 ML (monolayer) Fe coverage, isolated Fe nanoclusters are arranged in rows along the [110] direction. With increasing t_{Fe} the Fe clusters first connect along the [−110], but not along the [110] direction at 2.5 ML, then consist of percolated Fe clusters without a preferential orientation at 3 ML, and finally form a nearly smooth film at 4 ML coverage. Segregation of Ga atoms within the film and on the Fe surface appears to occur at t_{Fe}=4 ML, as evidenced by XPS. For coverages below the magnetic percolation, temperature-dependent *in situ* CEMS measurements in zero external field provided superparamagnetic blocking temperatures T_B of 62±5, 80±10, and 165±5 K for t_{Fe}=1.9, 2.2, and 2.5 ML, respectively. At $T<T_B$, freezing of superparamagnetic clusters is inferred from the observed quasilinear T dependence of the mean hyperfine magnetic field $\langle B_{hf}\rangle$. By combining the STM and CEMS results, we have determined a large magnetic anisotropy constant of $\sim 5\times 10^5$ and $\sim 8\times 10^5$ J/m^3 at t_{Fe}=1.9–2.2 and 2.5 ML, respectively. For $t_{Fe}\leqslant 2.5$ ML, our uncoated "free" Fe clusters exhibit intrinsic magnetic ordering below T_B, contrary to literature reports on metal-coated Fe clusters on GaAs. Our present results demonstrate that the nature of the percolation transition for free Fe nanoclusters on GaAs(001) in UHV is from superparamagnetism to ferromagnetism. From the Mössbauer spectral area, a very low Debye temperature Θ_D of 196±4 K is deduced for these uncoated Fe nanoclusters in UHV, indicating a strong phonon softening in the clusters.

DOI: 10.1103/PhysRevB.76.094403 PACS number(s): 76.80.+y, 75.75.+a, 61.46.−w, 75.20.−g

I. INTRODUCTION

The structural, magnetic, and electronic properties of Fe films deposited on GaAs have been studied extensively over the last decades and continue to attract strong interest.[1] Fe/GaAs is an interesting candidate among ferromagnet/semiconductor (SC) heterostructures for the realization of next-generation spintronic devices.[2–4] In fact, the Fe/GaAs-based hybrid system has been shown to be a promising device since it allows the manipulation of the SC spin polarization via electron spin injection from the FM.[5–12]

GaAs is an ideal substrate for the epitaxial growth of Fe(001) in the stable bcc phase since the lattice parameter of Fe is approximately half that of the zinc-blende-type GaAs ($2a_{Fe}/a_{GaAs}$=1.014, corresponding to a small lattice misfit of 1.4%). Nominally, this implies a small in-plane compressive stress for the Fe film. The achievement of single-crystal epitaxy is important since for many applications, one needs to exploit the magnetic anisotropy of the material. Therefore, amorphous, polycrystalline, or even oriented polycrystalline films are not acceptable.

High quality epitaxial growth of Fe on GaAs(001) and GaAs(110) substrates by molecular beam epitaxy (MBE) has been widely reported in the literature,[13–55] together with detailed investigations of the magnetic properties,[15–18,20–30,32–38,40–53] e.g., the evolution of the ferromagnetic order[22–25,32,40,45,48,51] or the relationship between uniaxial and cubic magnetic anisotropies as a function of layer thickness.[18,22,33,34,42–44,47,48,50,53] Some of these properties have been related to the interfacial compound formation and the atomic scale nucleation processes for various Ga- and As-terminated GaAs(100) substrate surface reconstructions.[19,21,23] Schönherr *et al.*[39] studied the growth of Fe on the (100), (311)*A*, and (331)*A* GaAs surfaces and its dependence on the growth temperature and termination of the GaAs surface, in an attempt to obtain macroscopically smooth Fe layers. They found that As-rich surfaces favored the formation of smooth Fe layers, if grown at low temperatures. Gordon *et al.*[31] showed that Fe films grown on an S-terminated surface exhibit a nearly cubic structure. By contrast, a tetragonal distortion was observed when deposited on the GaAs-(4×6) surface.

The successful growth of smooth epitaxial Fe layers with minimum interdiffusion at the Fe/GaAs interface is of relevance for the successful injection of highly spin-polarized electrons. The use of As-rich GaAs reconstructions has been shown to reduce the density of defects in the Fe layers.[39] It is also well known, however, that nonferromagnetic Fe-As compounds may form at the As-rich Fe/GaAs interface, producing interfacial "magnetic dead layers,"[26] or $Fe_3Ga_{2-x}As_x$ interlayers with only about half of the magnetization of bulk bcc-Fe (Refs. 28 and 29) due to the interdiffusion of As into the Fe overlayer. From such an interface, the injection of highly spin-polarized electrons into the semiconductor will become unlikely since a high spin polarization and large ferromagnetically ordered moments, even in the first metallic monolayers at the interface, are a necessary condition. Considerable efforts were devoted to gain insight into the effect of Ga and As interdiffusion across the Fe overlayer on the

magnetic properties and to explain the origin of the nonmagnetic layer occurring at the Fe/GaAs interface upon high-temperature Fe deposition.[36] Such interdiffusion was observed by several experimental techniques, including Auger electron spectroscopy and x-ray photoelectron spectroscopy.[15,20,30,35,36,43,51,56,57] The dissociation of Ga and As atoms from the surface of GaAs, followed by their outdiffusion across thin Fe layers, results in the formation of Fe-based alloys which critically alter the magnetic phase at the interface.[28–30] Meanwhile, several methods were explored to reduce the segregation of As onto the Fe surface. It is now established that the growth of the Fe film at or near room temperature (RT),[23,24,26,27,35] or at very low temperatures,[37] reduces the interdiffusion and interface roughness. Another possible way of reducing As interdiffusion and segregation of As to the surface is to grow the Fe films on Ga-rich surfaces.[23,26,27,35,41,52] In our previous works,[35,41,52] it was demonstrated by means of Mössbauer spectroscopy that it is possible to preserve a high Fe magnetic moment at the interface of epitaxial Fe/GaAs(001)-(4×6), Fe/GaAs(001)/$Al_{0.35}Ga_{0.65}As$(001), and Fe/GaAs(001)-based light-emitting diodes. Further, a bulklike Fe spin moment at the Fe/GaAs(100)-(4×6) interface was directly observed by x-ray magnetic circular dichroism.[46] By means of an appropriate selection of the growth parameters, the formation of nonmagnetic interfacial compounds can be avoided.

This paper focuses on the structural and magnetic properties of small Fe clusters epitaxially grown on GaAs(001)-(4×6). Although the epitaxial Fe/GaAs(001) system has been extensively studied, there is still a debate over the magnetic properties of the first few monolayers (MLs) and, in particular, over the critical Fe thickness for the onset of ferromagnetism. For example, ferromagnetism (FM) in Fe films grown at 175 °C on As-terminated GaAs(001)-(2×4) surfaces was reported to appear at RT at a critical coverage of 6 ML Fe.[22] For Fe films grown at RT on Ga-terminated GaAs(001)-(4×6) surfaces long-range-ordered FM at RT was observed by Xu *et al.*[23] at and above a thickness of about 5 ML Fe. Since in the initial state Fe on GaAs(001) is known to grow at RT in the Volmer-Weber mode [i.e., by nucleation of isolated three-dimensional (3D) islands], the Fe film is discontinuous until a certain coverage is reached, where island coalescence occurs. Based on magneto-optic Kerr effect (MOKE) measurements, Xu *et al.*[23] suggested that Fe growth at RT proceeds from a "nonmagnetic" Fe phase for the first 3.5 ML Fe to a short-range-ordered FM (superparamagnetic) phase up to about 5 ML Fe coverage, followed by FM above 5 ML Fe. Freeland *et al.*[25] obtained a critical value of 3.8 ML from MOKE susceptibility measurements, while Bensch *et al.*[32] reported a similar critical value of 3.6 ML Fe coverage, obtained from MOKE ac-susceptibility measurements. A crucial question is whether a local ferromagnetic order exists before the onset of the long-range-ordered FM phase. Bensch *et al.*[32] claimed that during the initial stages of Fe growth on GaAs(001), islands are formed that are smaller than the superparamagnetic limit until they coalesce. In principle, the onset of FM may be triggered by a superparamagnetism to FM transition or by a phase transition from nonferromagnetic (i.e., paramagnetic) state to FM.[32] Thus, the magnetic response before the onset of FM could originate either from paramagnetism (as Bensch *et al.* proposed in Ref. 32) or from superparamagnetism of Fe islands (as suggested by Xu *et al.*,[23] Freeland *et al.*,[25] and Steinmüller *et al.*[45]). The absence of magnetization at RT for coverages below ≈3.5 ML may, in principle, be caused by interfacial intermixing of Fe with As and Ga (dilute Fe-alloy formation), reducing the Curie temperature T_c to below RT), the formation of interfacial nonferromagnetic compounds, or superparamagnetism. Also, the coating material (Au, Al, or Cr) used by many researchers to protect their Fe films from oxidation during *ex situ* studies might have an influence on the magnetism of ultrathin Fe layers via interfacial intermixing. Therefore, the investigation of uncoated ("free") Fe/GaAs(001) ultrathin films in UHV is very important. Although a number of reports on *in situ* ultrahigh vacuum (UHV) room-temperature studies on uncoated Fe/GaAs(001) films exist,[18,21–25,38,45,51] *in situ* investigations performed at low temperatures (near or at magnetic saturation) are scarce.[53]

In the present work, we have investigated the magnetic properties of uncoated (free) Fe clusters on Ga-terminated GaAs(001)-(4×6) surfaces at 1.9, 2.2, and 2.5 ML Fe coverages by *in situ* conversion electron Mössbauer spectroscopy (CEMS) in UHV in the temperature range between 27 K and RT. These coverages are below the critical Fe coverage for ferromagnetism. Moreover, *in situ* scanning tunneling microscopy (STM), x-ray photoelectron spectroscopy (XPS), and reflection high-energy electron diffraction (RHEED) measurements provided information on cluster growth, atomic interdiffusion, and film structure, respectively. The present results allow us to clarify the nature of the percolation transition observed for uncoated ultrathin epitaxial Fe films on GaAs(001) in UHV.

II. EXPERIMENT

For the preparation and *in situ* investigation of our samples, we have used two independent UHV systems for MBE called UHV-1 and UHV-2. Details on the epitaxial growth of ultrathin Fe(001) films on GaAs(001)-(4×6) are given in our previous articles.[35,41,52]

STM and XPS measurements were carried out in system UHV-1 at Orlando, a UHV system equipped with three interconnected chambers that allows *in situ* sample preparation and multitechnique characterization. The substrates used in these experiments are pieces of an undoped "epiready" GaAs(001) wafer (purchased from Wafer Technology Ltd). The substrates were cleaned by acetone, followed by 2-propanol before being transferred into the MBE system (base pressure in the low 10^{-10} mbar range). The substrates were then annealed in UHV at 590 °C for 20 min to remove adsorbed impurities and the native oxide from the surface. Subsequently, the temperature was increased to 600 °C and maintained while the first cycle of Ar^+ ion sputtering was performed at an energy of 0.5 keV for 90 min. This sputtering cycle was followed by annealing at 600 °C for 30 min for optimum surface healing. This treatment was repeated

twice, whereupon the complete removal of oxygen and carbon was observed by XPS. Under similar preparation conditions, but on doped GaAs(001), Moosbühler *et al.*[33] and Ionescu *et al.*[49] observed by STM large terraces (more than 50 nm long and 50 nm wide) with ordered Ga-terminated (4×2) and (2×6) reconstructions. A mixture of (4×2) and (2×6) reconstructions has also been observed by STM on RT-sputtered and subsequently annealed GaAs(001) surfaces.[58,59] High-purity Fe was deposited nominally at RT and at a pressure better than 6×10^{-10} mbar using an e-beam evaporator with a constant rate of 0.05 Å/s, as monitored by a calibrated quartz crystal microbalance. Finally, the sample was transferred *in situ* to the STM chamber (pressure in the high 10^{-11} mbar range), where STM measurements were performed at RT using an etched W tip previously cleaned by Ar^+ ion sputtering. The STM images were acquired at constant current mode with the voltage applied to the sample.

RHEED, low-energy electron diffraction (LEED), Auger electron spectroscopy (AES), and ^{57}Fe CEMS were performed *in situ* in UHV in the MBE chamber of the UHV-2 system at Duisburg (base pressure $\leqslant1.4\times10^{-10}$ mbar). The GaAs(001) substrates used in these experiments had identical characteristics to the ones described above and were cleaned in an analogous way. After this treatment, no surface impurities were detected by AES, and a RHEED image typical of the "pseudo-(4×6)" reconstruction of the Ga-terminated GaAs(001) surface was observed (see below). Immediately after surface cleaning, the Mössbauer-active ^{57}Fe isotope (95.5% isotopical enrichment, 99.95 at. % purity) was deposited nominally at RT from a Knudsen cell (Al_2O_3 crucible) at a pressure $p\leqslant1.5\times10^{-9}$ mbar. However, the real substrate temperature during growth, T_s, was ~40–50 °C, as measured by a thermocouple fixed to the sample holder. The deposition rate (0.02–0.03 Å/s) and film thickness were monitored with a quartz crystal microbalance, which had been calibrated shortly before the preparation by RHEED intensity oscillations during the epitaxial growth of a fcc-Fe(001) thin film on a clean Cu(001) surface at RT.[60] Also, RHEED intensity oscillations observed above a coverage of ~5 ML of the growing Fe(001) film on GaAs(001)-(4×6) have been used for thickness calibration. The precision of this thickness determination is estimated to be 10%. During Fe growth RHEED images were continuously monitored by a charge coupled device camera and occasionally supported by LEED images. After preparation and structural characterization by RHEED and/or LEED, the sample was *in situ* transferred and attached to the cold finger of a UHV-compatible liquid-helium cryostat for ^{57}Fe CEMS in the temperature range between 27 K and RT in a zero-external field. A ^{57}Co source (Rh matrix) of ~100 mCi activity was mounted on the Mössbauer drive outside the UHV system. The γ radiation passed through a UHV-tight, high-purity Be window and hit the sample at perpendicular incidence relative to the film plane. A channeltron was used to detect the conversion electrons emitted from the sample surface during the Mössbauer resonance.

After the CEMS measurements in UHV, the ^{57}Fe films were coated by a protective Pt cap layer of 40 Å (grown at a rate of 0.04 Å/s at RT and evaporated from an electron gun). Subsequently, the Pt-coated samples were investigated *ex situ* by CEMS at RT. Throughout our paper, the temperature of 300 K represents room temperature. A proportional counter filled with high-purity He-4 %CH_4 gas with the sample mounted inside was employed for *ex situ* CEMS at RT. The γ-ray direction was perpendicular to the sample surface. The proportional counter could be placed between the poles of an electromagnet in order to acquire CEM spectra at RT in an external magnetic field oriented within the sample plane. The CEM spectra were fitted using a least-squares method by the program NORMOS by Brand.[61]

III. RESULTS AND DISCUSSION

A. Growth and structural properties

1. Low-energy electron diffraction and reflection high-energy electron diffraction

Details on the epitaxial growth of ultrathin Fe(001) films on GaAs(001)-(4×6) are given in our previous articles.[35,41,52] In our previous RHEED studies, we observed the disappearance of the GaAs(001)-(4×6)-surface reconstruction after deposition of 5.5 ML of Fe, and the appearance of a (1×1) pattern was observed up to a coverage of 42 ML. Our present investigations support and extend our earlier observations. Typical LEED and RHEED patterns of the clean GaAs(001)-(4×6) substrate are shown in Figs. 1(a)–1(d). These diffraction patters are characteristic of the pseudo-(4×6) reconstruction [with mixed (4×2) and (2×6) reconstructions] of the clean Ga-terminated GaAs(001) surface. A schematic of the LEED pattern is shown in Fig. 1(b), where the fundamental (superstructure) reflections are indicated by large (small) circles. Our present diffraction results are in agreement with the work by Zölfl *et al.*[26] and Madami *et al.*[47] and with our previous work.[35,41,52]

RHEED patterns taken at different Fe coverages are shown in Figs. 1(d) and 1(f)–1(j). After the initial Fe deposition [Figs. 1(d) and 1(f)–1(h)], i.e., at Fe coverages up to 3.6 ML, the GaAs superstructure reflections disappear, but the fundamental reflections are still observable, although they fade with increasing coverage until they disappear at 3.6–4 ML Fe coverages. This demonstrates that an incomplete island-like Fe film is formed, consisting of Fe nanoclusters. No reflections of bcc-Fe are seen up to ~3.1 ML Fe. This could indicate that thinner Fe films grow in a structurally disordered (amorphous) state, as mentioned by Bensch *et al.*[34] At 3.1 ML coverage, weak indications of bcc-Fe(001) reflections appear, superimposed on weak fundamental GaAs(001) diffraction spots. The GaAs(001) reflections disappear at ~3.6–4.0 ML Fe, while the bcc-Fe streaks increase in intensity [Fig. 1(i)]. The type of diffraction pattern observed for Fe in the range of ~3.6–4.0 ML indicates epitaxial, 3D Fe(001) island growth.[35] Above 4 ML Fe coverage, the Fe reflections gain in intensity, indicating the formation of a closed Fe film covering the entire substrate. Thus, coalescence of Fe clusters occurs at ~3.6–4.0 ML, and after 5 ML no significant change in the RHEED pattern was observed. This is demonstrated in the RHEED pattern of 93 ML Fe(001) [Fig. 1(j)], which is the typical 3D diffraction

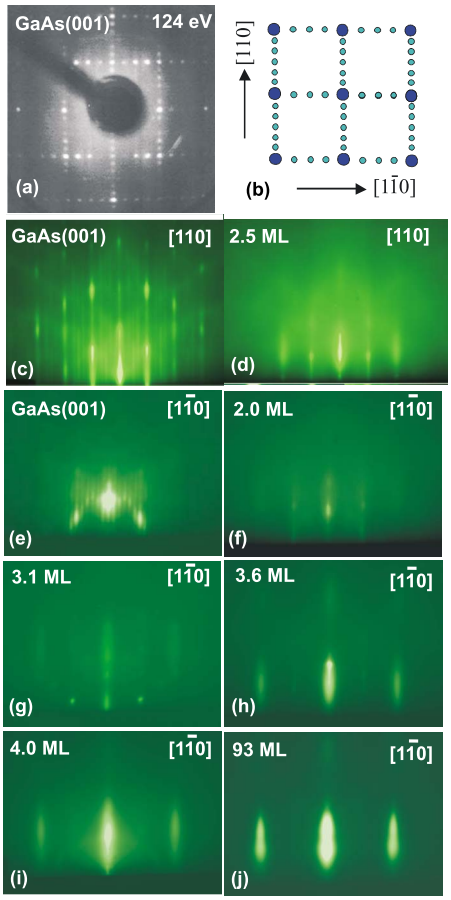

FIG. 1. (Color online) (a) LEED pattern of the clean GaAs(001)-(4×6) surface measured with 124 eV electron energy. (b) Schematics of the LEED diffraction spots of the GaAs(001)-(4×6) surface reconstruction. Images (c) and (d) display RHEED patterns measured with the electron beam along the [110] azimuthal direction of the clean and 2.2 ML Fe covered GaAs(001) surface, respectively. RHEED patterns measured with the beam (e) along [1−10] of clean GaAs(001)-(4×6) and at Fe coverages of (f) 2 ML, (g) 3.1 ML, (h) 3.6 ML, (i) 4.0 ML, and (j) 93 ML (electron energy: 15 keV).

pattern of a surface being rough on an atomic scale. Above 5 ML coverage, RHEED intensity oscillations with 1 ML Fe(001) periodicity were observed with increasing coverage. The appearance of these oscillations suggests that a smoothing of the Fe surface and quasi-layer-by-layer type of Fe growth occurs on the smoothed surface formed after the coalescence of the Fe islands. These results (for growth at 40°–50°C) are in agreement with previous reports by Brockmann *et al.*[27] on RT grown Fe/GaAs(001) samples. They found by STM that the roughness amplitude of 1-2 ML in height remained unchanged with increasing Fe thickness, indicating a quasi-layer-by-layer growth mode which leaves the surface structure of the Fe films unchanged. For growth at 150 °C, however, Gester *et al.*[18] found pyramidlike structures and a step density which increased approximately linearly with film thickness.

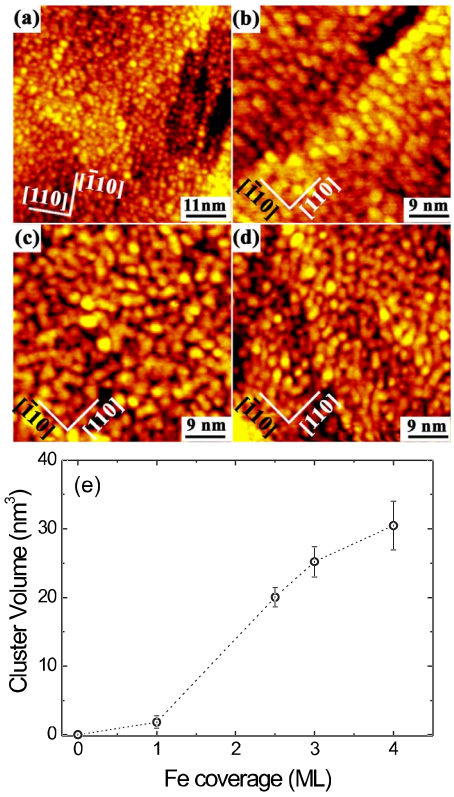

FIG. 2. (Color online) STM images of four different coverages of Fe on GaAs(001): (a) 1 ML, (b) 2.5 ML, (c) 3 ML, and (d) 4 ML. The tunneling parameters were (a) V_t=0.5 V, I_t=0.11 nA, (b) V_t=0.3 V, I_t=0.4 nA, (c) V_t=0.5 V, I_t=0.3 nA, and (d) V_t=0.32 V, I_t=0.31 nA. Fe clusters arranged parallel to the [−110] rows are observed for the (b) 2 ML Fe sample, while enhanced cluster percolation is observed when the Fe coverage is increased to (c) 3 ML and (d) 4 ML. (e) Average cluster volume obtained by STM as a function of Fe coverage.

2. Scanning tunneling microscopy and x-ray photoelectron spectroscopy

The structural growth of Fe on the GaAs(001) pseudo (4×6) surface was followed by *in situ* STM measurements. This surface exhibits domains of two different Ga-rich reconstructions [the Ga-rich (4×2) and the less Ga-rich (2×6) due to As termination[33,49,62–64]]. Figure 2 shows four STM images acquired on Fe/GaAs(001) surfaces and corresponding to thicknesses ranging from 1 to 4 ML. Figure 2(a) displays the arrangement of Fe after the deposition of 1 ML. Small Fe clusters ordered along parallel rows and separated by a distance of 1.6±0.2 nm can be observed among some random domains. This parallel arrangement is related to the nucleation of Fe clusters on top of As rows along the [110] direction that are characteristic of the GaAs(001)-(4×2) reconstruction, [Fig. 2(a), upper left part]. The typical distance between two As dimer rows in the (4×2) reconstruction corresponds to 1.6 nm.[33,49,62–64] At this coverage, round Fe clusters are observed. This growth is consistent with the presence of a Ga-rich surface where the diffusion of Fe monomers is energetically unfavorable.[49] At this coverage, a

single atomic step of the Fe domain, with a height of ~1.5±0.2 Å corresponding to one monolayer of bcc-Fe, can be observed. However, Fe clusters with 2 ML height (~2.9 Å) appear as well. This indicates the tendency of Fe to build Fe-Fe bonds instead of diffusing on top of Ga atoms. The growth of Fe is strongly influenced by the underlying reconstruction, leading to the nucleation of almost circular clusters with a height of 1–2 ML and arranged in rows along the [110] direction, in agreement with previous studies.[33,49]

The increase of the Fe coverage to 2.5 ML [Fig. 2(b)] leads to a more homogeneous size distribution of Fe clusters. Unlike the structure obtained in the case of 1 ML coverage, where the distribution is dominated by 1 ML high clusters (~1.5 Å), the Fe clusters in the 2.5 ML thick sample are mostly 2 ML high (~2.9 Å) and present larger diameters (~29.5±3.0 Å). This distribution suggests that the Fe clusters grow in lateral size once the 2 ML height has been reached. Besides, Fe clusters arrange into parallel lines separated by a distance of ~25.3 Å, which is close to the typical spacing (24 Å) between parallel As rows along the [−110] direction in the GaAs(001)-(2×6) reconstruction.[33,49,62–64] This arrangement is reminiscent of an initial GaAs(001)-(2×6) reconstruction where As rows represent the favorable nucleation sites for Fe atoms. In the early growth stages, the initial deposition of Fe atoms on As sites and in its vicinities (missing Ga dimers) is expected. Further increase in the coverage leads to a saturation in the diameter of the Fe clusters (~29 Å) along the [110] direction, while additional nucleation appears in the [−110] direction. As can be observed in the STM image of Fig. 2(b), Fe clusters appear connected along the [−110] direction as a result of the additional nucleation occurring when the diameter limit is attained. It is noteworthy that at this coverage (2.5 ML) no connectivity between Fe clusters is noticed along the [110] direction, suggesting that the onset of ferromagnetism at RT would not arise at this coverage.

Upon increasing the deposition to 3 ML, the surface morphology of this coverage consists of percolated Fe islands resulting from diffusion and coalescence of smaller Fe clusters [Fig. 2(c)]. At this thickness, the Fe domains are randomly distributed and the corresponding percolations exhibit no preferential orientation. Thus, the influence of the reconstruction is no longer observed at this coverage, suggesting a layer-by-layer growth with a surface roughness of 2 ML height (~2.9 Å). The growth of Fe from 2.5 to 3 ML takes place by the bridging of Fe atoms across Ga rows along the [110] direction when the initial reconstruction is (2×6) and along the [−110] orientation in the case of the (4×2) surface. The structural percolation of Fe domains is associated with the onset of the ferromagnetic phase, which is reported to occur at room temperature for a critical Fe thickness in the range of 3±0.5 ML to 4.8 ML (Refs. 23–25, 32, 40, 45, 48, and 51) on GaAs(001) surfaces. Increasing the coverage to 4 ML leads to a relatively smoothed surface compared to the previous 3 ML morphology, but with the same surface roughness of 2 ML height [Fig. 2(d)]. Similarly, Zölfl *et al.*[26] and Brockmann *et al.*[27] reported coalescence of Fe islands for a coverage between 3 and 4 ML followed by quasi-layer-by-layer growth after 5 ML Fe deposition on sputter-annealed Ga-rich GaAs(001) surfaces. Our STM results are in agreement with the conclusions drawn from our RHEED results described above.

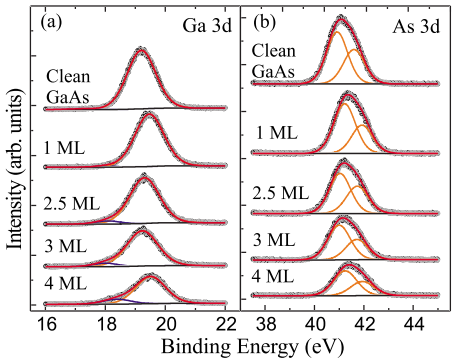

FIG. 3. (Color online) Ga 3*d* and As 3*d* core level photoelectron spectra as a function of Fe coverage. The spectra labeled "clean GaAs" were measured after the cleaning treatment described in the experimental section, leading to the GaAs(001)-(4×6) surface.

The effect of intermixing between the Fe overlayer and Ga and As atoms of the substrate was investigated by XPS measurements. Figure 3 shows peak intensities of the Ga 3*d* and As 3*d* core levels acquired after cleaning by sputtering and annealing the substrate and after the deposition of 1–4 ML of Fe. The binding energies (BEs) of 3*d* core levels of Ga and As ($3d_{5/2}$,$3d_{3/2}$) measured before Fe deposition are 19.2 eV and (40.9 eV,41.6 eV), respectively. Those values are in agreement with what has been previously obtained for a clean GaAs surface.[65] The deposition of 1 ML of Fe on this freshly prepared surface induced a moderate increase in the BE of both Ga and As 3*d* levels. This shift to higher BE with comparable values for Ga $3d_{5/2}$ (~0.26 eV) and As $3d_{5/2}$ (~0.30 eV) indicates a substantial change in their atomic coordination at the Fe/GaAs interface. The increase in the binding energy can be interpreted as a result of a downward band bending effect taking place at the GaAs(001) surface, which creates extrinsic surface states and a negatively charged GaAs(001)-Fe interface. This initial shift of the core level to a higher binding energy is commonly observed when a clean semiconductor surface is exposed to small amounts of metallic atoms (~1 ML coverage) due to charge transfer effects.[66]

Due to the low density of Fe clusters and the lack of Fe mobility at this coverage, the Fe-Fe coordination must be insignificant, resulting in predominantly Fe-GaAs interactions as the origin of the moderate shift in the BE of Ga and As 3*d* levels. As the thickness of Fe is increased to 2.5 ML, only slight shifts are observed in the BE of Ga 3*d* (~0.10 eV) and As $3d_{5/2}$ (0.15 eV) levels. This effect can be attributed to the increase of Fe-Fe coordination, which is energetically more favorable than Fe–Ga bonds, resulting in a significant reduction of the Fe-substrate interactions. The tendency of the 3*d* BE of Ga and As atoms at the interface to return to their original values before Fe deposition indicates the lack of stable Fe–Ga and Fe–As bonds. The absence of intermixing between As and Fe is evident if we consider the evolution of the XPS 3*d* levels in Fig. 3(b), where no shoul-

der at higher BE can be observed in the As $3d$ core level spectra characteristic of Fe–As. Such a shoulder has been observed for Fe on the As-rich GaAs(001)-$c(8\times2)$ surface and was attributed to interstitial As in the Fe overlayer.[56] We did not observe this effect here. Moreover, the BE of As $3d_{5/2}$ for coverages higher than 2.5 ML exhibits a remarkable stability. Thus, we infer that no diffusion of As into the Fe layer and no As segregation on the Fe surface occurs below 4 ML Fe. Reduced intermixing (relative to As-terminated surfaces) was previously reported for Ga-terminated surfaces where As is depleted from the surface prior to Fe deposition.[36] However, the diffusion of Ga atoms through the Fe overlayer becomes evident by the appearance of an additional peak in the XPS spectra at lower BE (18.0 eV) [Fig. 3(a)]. The measured BE corresponds to the value of a pure Ga ($3d_{5/2}$) level, indicating the presence of low-coordinated Ga atoms at the surface. The intensity of this shoulder in the XPS spectra was found to increase with increasing Fe thickness and can be attributed to Ga atoms diffusing to the surface of the Fe film. The diffusion of Ga atoms through Fe overlayers has been previously demonstrated.[51,56] However, segregation at the Fe surface is generally prevented by the presence of As. This effect can be understood in terms of energy minimization since based on the heats of formation for the Fe_2As and Fe_2Ga phases ($\Delta H_{Fe_2As}=-38$ kJ/mol and $\Delta H_{Fe_2Ga}=-16$ kJ/mol),[36] the Fe–As bond is more favorable than Fe–Ga. In our study, the segregation of Ga atoms at the Fe surface can take place since we did not observe any As diffusion that may inhibit such segregation process. This behavior was also theoretically predicted by Mirbt *et al.*[67] The attenuation of Ga and As intensities as a function of the Fe coverage gives further insight into this diffusion effect [Fig. 4(a)]. The attenuation of Ga and As $3d$ intensities exhibits slightly different trends, with the Ga signal decreasing more slowly than the As one. This effect can be attributed to the presence of dissolved Ga atoms in the Fe overlayers and on the surface of the topmost Fe layer, as predicted theoretically by Erwin *et al.*[68] and observed above 3 ML coverage by Giovanelli *et al.*[51]

Figure 4(b) (inset) shows the XPS spectra collected for the Fe $2p$ core level as a function of the coverage from 1 to 4 ML. For all Fe thicknesses, a similar binding energy of ~706.8 eV (Fe $2p_{3/2}$ level) is measured. This value is in agreement with what is expected for bulk Fe, indicating the stability of the chemical environment of Fe, even for the lowest Fe coverages investigated here and confirming the absence of strong Fe–Ga and Fe–As bonds. Since the magnetic moment in Fe is carried by $3d$ orbitals and those orbitals are usually involved in the interactions with other chemical species, the reduced intermixing detected in our samples indicates that those orbitals should have bulklike characteristics. Therefore, the onset of ferromagnetism is expected to occur at lower Fe thicknesses than if significant intermixing was involved. Then, this onset should mainly depend on the coalescence of the Fe islands, with a minimum influence of Fe-Ga and Fe-As intermixing. Our STM results reveal the beginning of Fe coalescence at ~2.5 ML (Fig. 2), with nearly complete cluster coarsening into domains when the Fe thickness is about 3 ML. The XPS results are in agreement

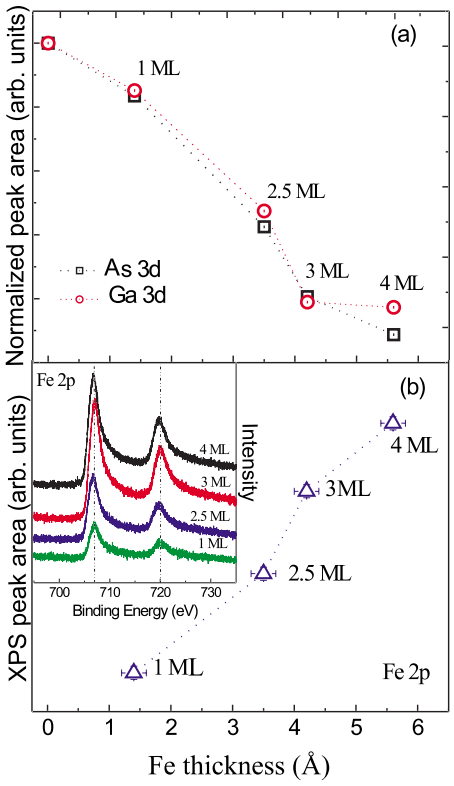

FIG. 4. (Color online) (a) Normalized integrated XPS signals from Ga $3d$ (circles) and As $3d$ (squares) measured *in situ* (UHV) as a function of Fe coverage on clean GaAs(001). The areas of the Ga and As peaks in the GaAs(001) substrate have been used for the normalization. (b) Integrated XPS signal of the Fe $2p$ core level (triangles) and raw Fe $2p$ XPS spectra (insert) measured as a function of Fe coverage on clean GaAs(001). (The dotted lines are a guide for the eye.)

with the morphology data since a clear increase of the Fe $2p$ intensities is observed from 1 to 3 ML coverages [Fig. 4(b)]. For an Fe thickness of ~3 ML, a change in the slope can be observed in the increase of the Fe $2p$ intensities, which is attributed to the effect of the coalescence of the Fe clusters: The contribution of Fe atoms from the surrounding small islands is screened by the topmost layer as the Fe clusters start coalescing. Additionally, the segregation of Ga atoms to the surface of the topmost Fe layer will reduce the Fe $2p$ intensity.

3. Mössbauer spectroscopy

Figure 5(a) displays CEM spectra measured at RT *in situ* in UHV (UHV-2) on ^{57}Fe(001)/GaAs(001) samples with 2.5, 2.2, and 1.9 ML ^{57}Fe coverages (from top to bottom, respectively). The spectra shown in Fig. 5(b) were taken *ex situ* at RT after coating the same Fe films with a 40 Å thick protective Pt film. All spectra in Fig. 5 were measured in zero-external field ($B_{ext}=0$ T), except the bottom spectrum in Fig. 5(b), which was obtained *ex situ* in an external field of $B_{ext}=1.3$ T applied in the film plane of the Pt-coated 1.9 ML ^{57}Fe sample. All spectra could be least-squares fitted with a slightly asymmetric quadrupole-split doublet, except the bot-

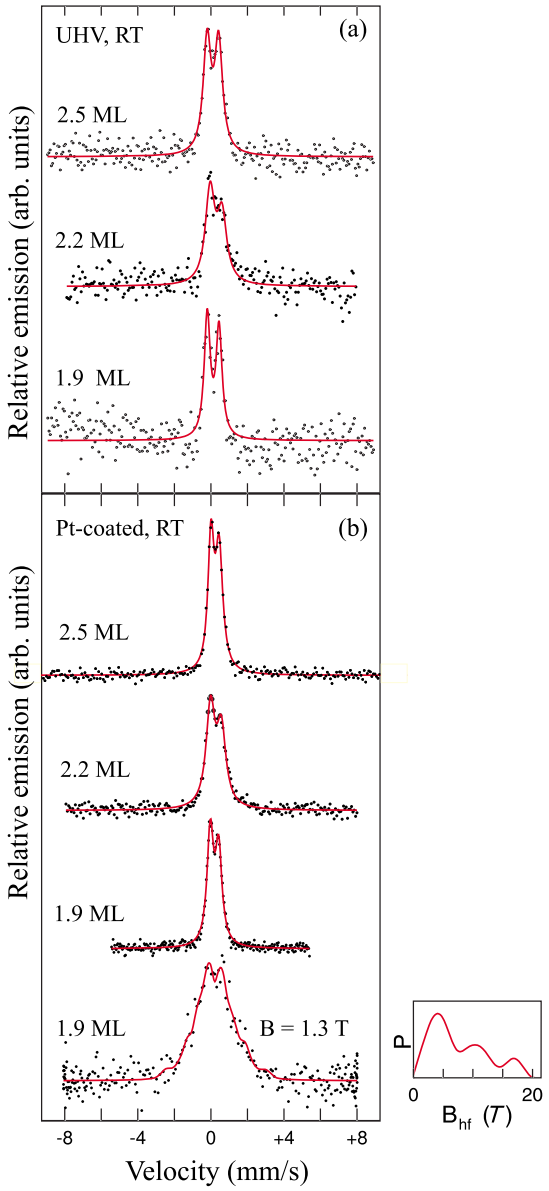

FIG. 5. (Color online) CEM spectra taken at room temperature on ^{57}Fe(001)/GaAs(001)-(4×6) for ^{57}Fe coverages of 2.5, 2.2, and 1.9 ML. (a) *in situ* in UHV (free ^{57}Fe surface) and (b) *ex situ* (Pt covered ^{57}Fe surface). Bottom spectrum in (b): 1.9 ML ^{57}Fe coverage measured *ex situ* in B_{ext}=1.3 T. (All other spectra were measured at B_{ext}=0 T.) The full-drawn line is a least-squares fit with a quadrupole doublet except in the bottom spectrum of (b), which is fitted according to a distribution of hyperfine fields $P(B_{hf})$ (right-hand side).

tom spectrum in Fig. 5(b). The Mössbauer parameters obtained from the fitting are given in Table I. The values of the isomer shift δ of all samples are found to be positive with respect to δ=0.0 mm/s of pure bulk bcc-Fe (our reference absorber), indicating a decrease of the *s*-electron density at the ^{57}Fe nucleus at the ^{57}Fe/GaAs(001) interface. This decrease of the *s*-electron density may arise from electronic hybridization of wave functions of Fe and neighboring As and/or Ga atoms, as well as from the expansion of the average Fe-Fe distance in the film (relative to that of bulk bcc-Fe at RT).[69] On average, the Pt coating resulted in an increase of the δ values by +0.04±0.05 mm/s relative to those of the uncoated Fe films. This indicates a further reduction of the *s*-electron density at the ^{57}Fe nucleus due to Pt.

The observed quadrupole splitting ΔE_Q of the doublet is relatively large for the uncoated Fe films ($\Delta E_Q \approx 0.64$ mm/s on the average, Table I) but is remarkably reduced (to an average value of $\Delta E_Q \approx 0.50$ mm/s) after Pt coating. The pure observation of an electric quadrupole splitting in Fig. 5 is a qualitative proof of the noncubic local environment around the ^{57}Fe atom in these ^{57}Fe nanoclusters on GaAs(001), whether free or Pt coated. One could think that the reason for this symmetry breaking is the small lattice mismatch of 1.4% between bcc-Fe and GaAs that would lead to a small in-plane lattice compression (and, consequently, to a lattice expansion along the film-normal direction) in the Fe nanoclusters. However, contrary to expectation, the in-plane atomic spacing in epitaxial Fe(001) films grown at 40–50 °C on GaAs(001) has been demonstrated by RHEED to *increase* up to 2.5% (relative to that of bulklike bcc-Fe films) for Fe coverages below 5 Å,[35] most likely due to some atomic intermixing at the Fe/GaAs interface. This in-plane expansion could result in a lattice *contraction* along the film-normal direction. Our XPS results (Sec. III A 2) suggest the presence of Ga impurities rather than As impurities on the surface of the Fe clusters. Since Ga atoms are larger than Fe atoms, the incorporation of Ga atoms in bcc-Fe at substitutional lattice sites can explain the observed increase of the atomic spacing in the nanoclusters. Positive isomer shifts (as given in Table I) are typically observed for $Fe_{1-x}Ga_x$ solid solutions.[70]

The slight asymmetry observed in the intensity of the two lines in the quadrupole doublets [Figs. 5(a) and 5(b)] proves that a preferred direction of the main component V_{zz} of the electric field gradient (EFG) exists in the epitaxial ^{57}Fe nanoclusters on GaAs(001). According to Table I, the average line intensity ratio A_{21} is equal to 0.83 and 0.86 mm/s [averaged over all Pt-coated and uncoated (UHV) nanoclusters, respectively]. For simplicity, we assume a uniaxial EFG with $V_{zz} \neq 0$ and a zero asymmetry parameter (η=0). Then, the average angle $\langle\varphi\rangle$ between the direction of V_{zz} and the γ-ray direction (or film-normal direction) can be determined from the ratio A_{21} of the integrated intensity of line 2 (with more positive velocity) and line 1 (with more negative velocity) according to the relation:[71]

$$A_{21} = \frac{\frac{2}{3} + \sin^2\varphi}{1 + \cos^2\varphi} \quad \text{or} \quad A_{21} = \frac{1 + \cos^2\varphi}{\frac{2}{3} + \sin^2\varphi} \tag{1}$$

for $V_{zz}<0$ or $V_{zz}>0$, respectively. By using the average values of A_{21}=0.86 and 0.83 for all uncoated (UHV) and all Pt-coated samples, respectively, we obtain from Eq. (1) values of $\langle\varphi\rangle$=61° and 63° for ^{57}Fe/GaAs(001) and Pt/^{57}Fe/GaAs(001), respectively, assuming $V_{zz}>0$ (average angle of 62°). If we assume $V_{zz}<0$, the $\langle\varphi\rangle$ values are 49° and 47° for ^{57}Fe/GaAs(001) and Pt/^{57}Fe/GaAs(001), re-

TABLE I. ^{57}Fe Mössbauer parameters measured at room temperature: isomer shift δ (relative to bulk bcc-Fe at RT), quadrupole splitting ΔE_Q, Lorentzian linewidth Γ (full width at half maximum) of the Lorentzian line, ratio of the spectral areas of lines 2 and 1, A_{21}, quadrupole nuclear line shift 2ε, average hyperfine field $\langle B_{hf}\rangle$, and root mean square (rms) of $P(B_{hf})$ distribution. The data are extracted from Fig. 5.

T=RT	Isomer shift δ (mm/s)	Quadrupole splitting ΔE_Q (mm/s)	Lorentzian linewidth Γ (mm/s)	Line intensity ratio A_{21}
		^{57}Fe (2.5 ML)/GaAs(001)		
As deposited B_{ext}=0 T, *in situ*	0.25±0.01	0.63±0.02	0.52±0.03	0.98±0.07
Pt (40 Å) coated B_{ext}=0 T, *ex situ*	0.312±0.004	0.447±0.006	0.44±0.01	0.89±0.03
		^{57}Fe (2.2 ML)/GaAs(001)		
As deposited B_{ext}=0 T, *in situ*	0.36±0.01	0.65±0.02	0.62±0.03	0.72±0.07
Pt (40 Å) coated B_{ext}=0 T, *ex situ*	0.35±0.01	0.59±0.01	0.59±0.02	0.76±0.04
		^{57}Fe (1.9 ML)/GaAs(001)		
As deposited B_{ext}=0 T, *in situ*	0.25±0.01	0.65±0.02	0.40±0.03	0.89±0.08
Pt (40 Å) coated B_{ext}=0 T, *ex situ*	0.32±0.01	0.46±0.01	0.43±0.01	0.83±0.02
Pt (40 Å) coated B_{ext}=1.3 T, *ex situ*	0.35±0.04	2ε= −0.022±0.08	average $\langle B_{hf}\rangle$ 7.6±0.3 T	rms B_{hf} 6.3 T

spectively (average angle of 48°). V_{zz} is canted relative to the film-normal direction by these angles. Unfortunately, the sign of V_{zz} is unknown; it can be determined, in principle, by applying a strong magnetic field.

Irrespective of the unknown sign of V_{zz}, the $\langle\varphi\rangle$ values obtained provide evidence for a significant in-plane component of V_{zz}. Two reasons may be responsible for this phenomenon: (i) a preferred noncubic atomic environment of Ga atoms (less likely As atoms, as our XPS results show) around the ^{57}Fe atom in the intermixed interfacial region (as opposed to a random interfacial alloy) and/or (ii) an anisotropic in-plane lattice distortion superimposed to the tetragonal distortion along the film-normal direction. Such an in-plane lattice strain has been made responsible for the observed strong uniaxial magnetic anisotropy in the thin epitaxial Fe films on GaAs(001) in a recent theory,[67] and was observed experimentally.[55] Future angular dependent CEMS studies at grazing incidence of the γ ray could provide information about the preferred direction of the in-plane component V_{zz}.

B. Magnetic properties

1. Room temperature

An open question is whether the ^{57}Fe nanoclusters on GaAs(001) at RT are either in a paramagnetic state, or in a superparamagnetic state above the blocking temperature T_B (or, alternatively, in a state of thermally fluctuating spin clusters above a critical magnetic ordering temperature T_C). While the paramagnetic state will respond only very weakly to an external field B_{ext}, the superparamagnetic state (above T_B) or the state of correlated spin fluctuations (above T_C), may show a strong response to B_{ext}. The external field will block the rapid thermal superparamagnetic fluctuations (or the thermal fluctuations of spin clusters above T_C) and cause the appearance of a Zeeman sextet with a relatively large hyperfine field splitting.[72,73] On the other hand, the Mössbauer spectrum in the case of paramagnetism will be only weakly affected by B_{ext}.

Figure 5(b) (bottom spectrum) shows the result of an *ex situ* CEMS measurement at RT with the Pt-coated 1.9 ML ^{57}Fe/GaAs(001) sample placed in a field B_{ext} of 1.3 T. The drastic broadening observed for this in-field spectrum, as compared to the zero-field spectrum for the same 1.9 ML ^{57}Fe sample, unambiguously demonstrates the presence of a relatively large effective hyperfine magnetic field induced by the external field via slowing down of superparamagnetic fluctuations or critical fluctuations of spin clusters. The Mössbauer parameters obtained from spectral least-squares fitting with a distribution of hyperfine magnetic fields $P(B_{hf})$ [Fig. 5(c), bottom spectrum, right-hand side] are shown in Table I (bottom row). The distribution of hyperfine fields can be the result of both the cluster size distribution and the alloy formation near the Fe/GaAs interface. The most striking feature is the relatively large average (effective) hyperfine field $\langle B_{hf}\rangle$ of 7.6 T induced by the much smaller external field of 1.3 T. This proves that the ^{57}Fe nanoclusters in the 1.9 ML ^{57}Fe/GaAs(001) sample (which have the smallest average

cluster size in all our samples) are either superparamagnetic at RT or show critical spin-cluster fluctuations at RT $> T_C$. Paramagnetism can be definitively ruled out at RT because in that case the measured (effective) hyperfine field would be about equal to the external field. We may conclude that also the ^{57}Fe clusters in the 2.2 and 2.5 ML ^{57}Fe/GaAs(001) samples (containing larger clusters) are superparamagnetic (or show critical spin-cluster fluctuations) at RT. Similar CEM spectra on the latter samples, taken at RT and in an external field (not shown), exhibit analogous broadening effects as the one shown in Fig. 5(b) (bottom spectrum).

The magnitude of the measured (effective) average hyperfine field $\langle B_{hf}\rangle$ is given by $\langle B_{hf}\rangle = \langle B_{int}\rangle - B_{ext}$, where $\langle B_{int}\rangle$ is the magnitude of the average intrinsic hyperfine field (assuming collinearity of all fields as in a ferromagnet). Using $B_{ext}=1.3$ T and $\langle B_{hf}\rangle = 7.6$ T, we obtain a value of $\langle B_{int}\rangle = 8.9$ T for the nanoclusters at RT. This value should be compared with $\langle B_{int}\rangle = 33.0$ T for bulk bcc-Fe at RT. The main factor responsible for the smaller $\langle B_{int}\rangle$ value observed in the nanoclusters is the incomplete blocking of the superparamagnetic or thermal spin-cluster fluctuations by the relatively weak external field; i.e., a complete static spin alignment along B_{ext} is not yet achieved. Other factors include alloying effects and nanocluster size effects.

Although it is possible to exclude paramagnetism at RT from a Mössbauer measurement in an external field, such a measurement cannot distinguish between superparamagnetic fluctuations ($T > T_B$) and critical fluctuations of spin clusters ($T > T_C$). However, we will show below that the measured T dependence of the average hyperfine magnetic field $\langle B_{hf}\rangle$ provides strong evidence of superparamagnetism and *not* of critical fluctuations of spin clusters near a phase transition.

2. Low temperature

Figures 6–8 display CEM spectra from uncoated ^{57}Fe/GaAs(001) samples at 1.9, 2.2, and 2.5 ML ^{57}Fe coverages, respectively. The spectra were measured *in situ* in UHV-2, in zero-external field, as a function of temperature from 27 K to RT. At RT, the CEM spectra consist of the central quadrupole-split doublet due to superparamagnetism, as described above. With decreasing temperature, the overall width of the spectra first increases only slightly until below a certain temperature a drastic broadening occurs due to a sudden onset of magnetic hyperfine splitting. This behavior indicates a transition from superparamagnetism to ferromagnetism of the Fe clusters in all three samples upon cooling, as will be outlined in more detail below. Since the thermal fluctuations of the net magnetization in a superparamagnetic cluster are faster than the Mössbauer observation time (being equal to the Larmor precession time of $\sim 10^{-8}$ s of the ^{57}Fe nuclear magnetic moment), the time-averaged hyperfine field measured in the superparamagnetic state (i.e., for temperatures above the blocking temperature T_B) by the Mössbauer effect in the absence of an external magnetic field becomes zero, and the effect is insensitive to the internal (local) ferromagnetic order within the Fe clusters. In Figs. 6–8, at the lowest temperature, i.e., in the ferromagnetic state, magnetic hyperfine-split spectra are observed for all samples due to the

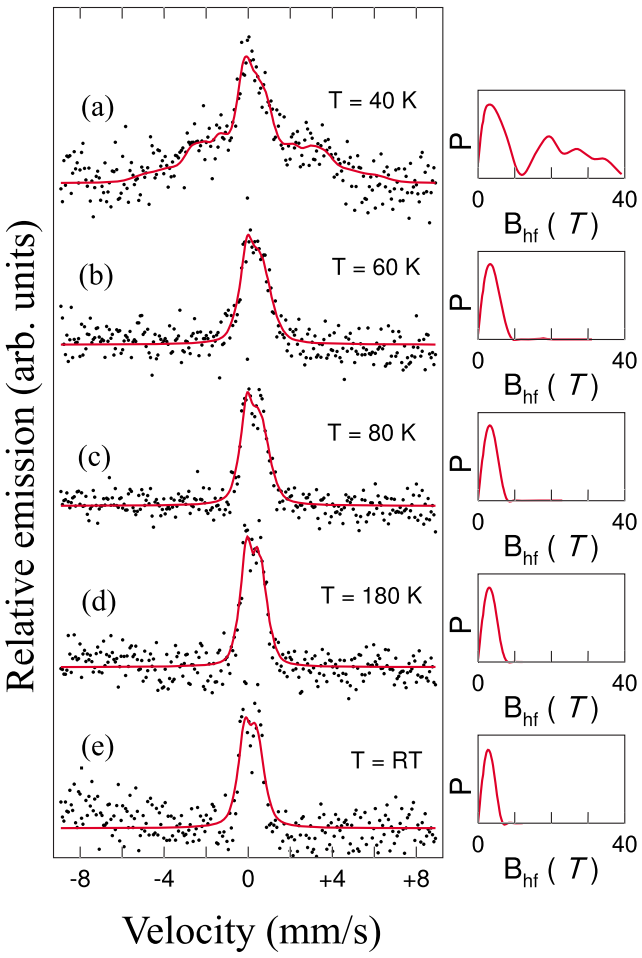

FIG. 6. (Color online) CEM spectra and hyperfine-field distributions $P(B_{hf})$ (right) of a discontinuous ^{57}Fe(001) film of 1.9 ML coverage grown on GaAs(001)-(4×6) and measured in zero-external field *in situ* in UHV at a temperature of (a) 40 K, (b) 60 K, (c) 80 K, (d) 180 K, and (e) room temperature.

freezing of the superparamagnetic relaxations. It is remarkable that the low-T spectra measured do not show sharp lines but are smeared out, very likely due to a distribution of various properties such as cluster sizes, relaxation times, hyperfine magnetic fields, superparamagnetic blocking temperatures T_B, and Curie temperatures. Therefore, the detailed theoretical description of the measured spectra in Figs. 6–8 is a difficult task.

In order to determine the average superparamagnetic blocking temperature and the average hyperfine field from the spectra, it is sufficient to least-squares fit all spectra in Figs. 6–8 with a magnetic hyperfine-field distribution $P(B_{hf})$. For this fitting we assumed in-plane Fe magnetic moments, implying a line intensity ratio in the basic Zeeman sextets of distribution of $I_{23}=I_{54}=4.0$ [where $I_{23}(I_{54})$ is the line intensity ratio of line 2 (line 5) to line 3 (line 4)]. The $P(B_{hf})$ distributions obtained from the fitting are shown in Figs. 6–8 (right-hand side).

At RT, the real CEM spectra of the superparamagnetic Fe clusters consist of the quadrupole-split doublets described in Sec. III A 3). However, in order to obtain a quantitative mea-

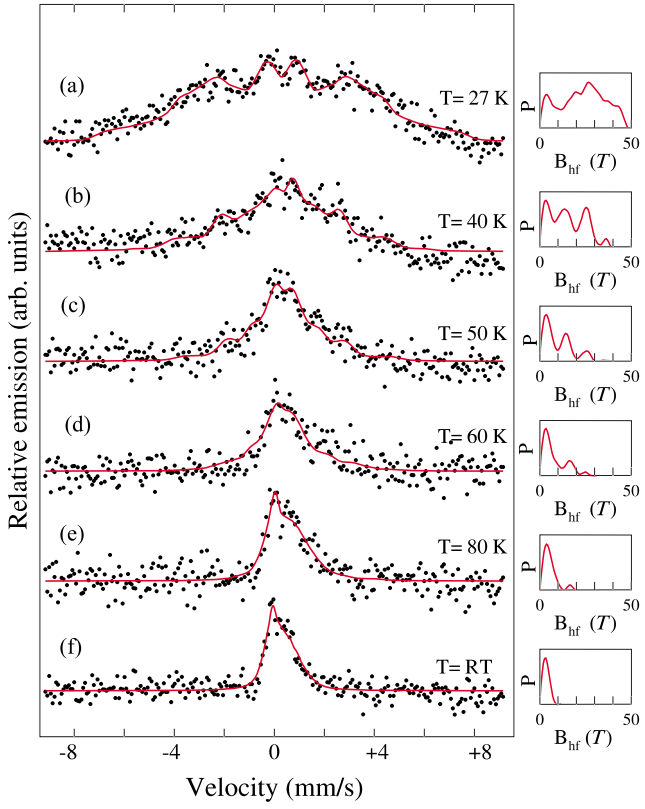

FIG. 7. (Color online) CEM spectra and hyperfine-field distributions $P(B_{hf})$ (right) of a discontinuous ^{57}Fe(001) film of 2.2 ML coverage grown on GaAs(001)-(4×6) and measured in zero external field *in situ* in UHV at a temperature of (a) 27 K, (b) 40 K, (c) 50 K, (d) 60 K, (e) 80 K, and (f) room temperature.

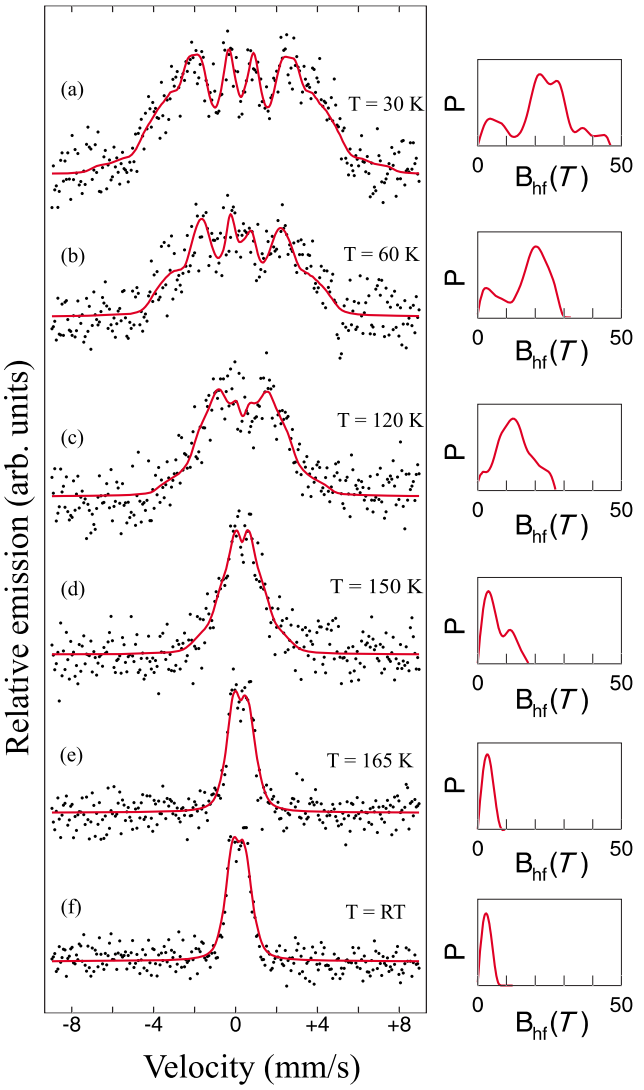

FIG. 8. (Color online) CEM spectra and hyperfine-field distributions $P(B_{hf})$ (right) of a discontinuous ^{57}Fe(001) film of 2.5 ML coverage grown on GaAs(001)-(4×6) and measured in zero-external field *in situ* in UHV directly after deposition at a temperature of (a) 30 K, (b) 60 K, (c) 120 K, (d) 150 K, (e) 165 K, and (f) room temperature.

sure of the extra spectral broadening and of the average hyperfine field causing this broadening, we have consistently fitted all spectra in Figs. 6–8 (including those at RT) with a distribution $P(B_{hf})$. The fictitious $P(B_{hf})$ distributions of the Fe clusters at RT [bottom spectra in Figs. 6–8] show a dominant peak near a zero hyperfine field, representing the superparamagnetic state. With decreasing T, the hyperfine-field distributions become systematically broader.[74]

Figure 9(a) displays the T dependence of the root-mean-square (rms) width of the distribution $P(B_{hf})$ for ^{57}Fe/GaAs at ^{57}Fe coverages of 1.9 ML (triangles), 2.2 ML (full circles), and 2.5 ML (full squares). The data points have been obtained from Figs. 6–8. More precisely, we have plotted the excess rms width (or corrected rms width) relative to the rms width of the distribution at RT for each sample, where we know the Fe clusters to be superparamagnetic. (At RT, rms =2.8, 3.1, and 3.2 T for 1.9, 2.2, and 2.5 ML Fe, respectively). One can notice that upon cooling from RT, the rms width first increases only very weakly, but then shows a remarkably abrupt and drastic rise at a certain temperature specific for each sample. We identify this temperature as the superparamagnetic blocking temperature T_B of the different samples.[75] From the intersections of the linear fittings to the data points [dashed lines in Fig. 9(a)], we infer blocking temperatures of 62±5 and 165±5 K for ^{57}Fe coverages of 1.9 and 2.5 ML, respectively. For 2.2 ML ^{57}Fe coverage, the transition appears to be less sharp and more rounded, starting as low as ~80 K upon cooling. We estimate T_B as 80±10 K.

The T dependence of the average hyperfine field $\langle B_{hf}\rangle$ of the different samples is shown in Fig. 9(b). The data points have been obtained from the $P(B_{hf})$ distributions shown in Figs. 6–8. To be more precise, in Fig. 9(b) we have plotted the excess average hyperfine field (or corrected average $\langle B_{hf}\rangle$) relative to the (fictitious) average hyperfine field for each sample at RT, where the Fe clusters are superparamagnetic. (This fictitious average hyperfine field at RT was found to be 3.1, 3.6, and 3.2 T for 1.9, 2.2, and 2.5 ML Fe, respectively.)

A comparison of Figs. 9(a) and 9(b) shows that the T dependence of the corrected rms and the corrected $\langle B_{hf}\rangle$ is very similar. Again, we identify the superparamagnetic blocking temperature as the temperature at which the hyper-

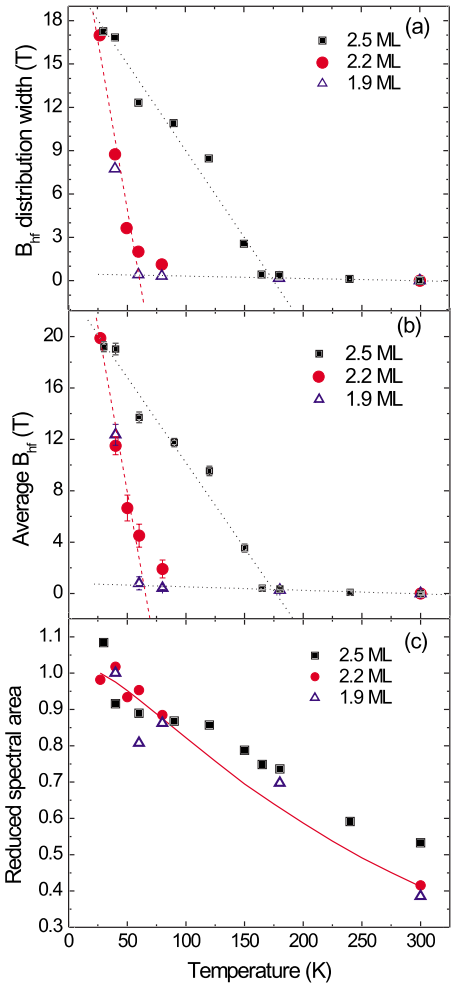

FIG. 9. (Color online) Temperature dependence of (a) measured excess root-mean-square width of the hyperfine-field distribution $P(B_{hf})$ (relative to that at RT), (b) measured excess average magnetic hyperfine field $\langle B_{hf}\rangle$ (relative to that at room temperature), and (c) measured reduced spectral area. The ^{57}Fe(001) coverages are 2.5 ML (full squares), 2.2 ML (full circles), and 1.9 ML (open triangles). The full-drawn line in (c) shows the normalized Debye-Waller factor (f factor) (normalized by the average f value between 27 and 40 K) calculated according to the Debye model for Θ_D =196 K. All measured quantities were obtained from Figs. 6–8. The dotted lines in (a) and (b) are a guide for the eye.

fine field falls to zero.[75] From the intersections of linear fittings to the data points in Fig. 9(b), we obtain blocking temperatures of 62±5 and 165±5 K for 1.9 and 2.5 ML ^{57}Fe coverages, respectively, in agreement with the T_B values inferred from Fig. 9(a). According to the data points for 2.2 ML coverage, the transition for this sample is again found to be less sharp and appears to start at ~80 K upon cooling, with T_B estimated to be 80±10 K.

3. Superparamagnetism

We now return to the question whether our uncoated ^{57}Fe nanoclusters on GaAs(001)-(4×6) in UHV show superparamagnetic behavior with a blocking temperature T_B or whether the temperature labeled T_B in reality is a critical temperature (magnetic ordering temperature T_C) indicative of a ferromagnetic phase transition. Bensch *et al.*[32] have argued that the onset of ferromagnetism below a certain temperature at a certain critical Fe coverage in the ultrathin regimes of Fe/GaAs(001)-(4×2) and (2×6) is related to a two-dimensional (2D) phase transition. Based on MOKE measurements performed *ex situ* on an Au-coated wedge-shaped Fe film, Bensch *et al.*[32] could describe the T dependence of the remanent Kerr rotation by a power law $M_S \propto (1-T/T_C)^{\beta}$ with a critical exponent β=0.26, as expected for 2D XY systems of finite size (M_S=spontaneous magnetization). However, our zero-field *in situ* CEMS results in UHV on single-layer Fe films on GaAs(001)-(4×6) are at odds with the findings of Bensch *et al.* The striking *quasilinear* temperature dependence of the average hyperfine field $\langle B_{hf}\rangle$ observed for $T \leqslant T_B$ on our ultrathin uncapped Fe films by CEMS [Fig. 9(b)] is not characteristic of a magnetic phase transition but rather provides strong evidence for a superparamagnetic transition. Under no circumstances can our data points for 2.5 and 2.2 ML ^{57}Fe coverage, [Fig. 9(b)] be described by the power law of a 2D (or 3D) magnetic phase transition. For 1.9 ML Fe coverage, we do not have enough data points to give a conclusive answer, but the data points are consistent with those at 2.2 ML coverage.

Our interpretation of the quasilinear T dependence of $\langle B_{hf}\rangle$ in terms of a superparamagnetic transition is strongly supported by *ex situ* superconducting quantum interference device (SQUID) measurements of the remanent magnetization M_R versus T of Al-coated Fe/GaAs(001) films at 3.0–3.5 ML Fe coverage (i.e., just below the critical coverage for coalescence), reported by Herfort *et al.*[48] One can notice in Fig. 4 of that work[48] that $M_R(T)$ follows approximately a linear T dependence below the transition temperature, whereby the range of this linear behavior increases by reducing the Fe thickness from 3.5 to 3.0 ML. Simultaneously, the magnetic ordering temperature was observed to decrease with decreasing Fe coverage.[48] This behavior can be understood by the nucleation and growth of Fe islands at the initial stages of growth. With decreasing Fe coverage, away from the critical value for coalescence, the fraction of isolated Fe clusters in the film, which are superparamagnetic, increases. This leads to the appearance of the approximately linear sections of $M_R(T)$ below the ordering temperature, with the linear range being more extended if the Fe coverage is further below the thickness for coalescence. Our interpretation of the quasilinear $\langle B_{hf}\rangle$ versus T behavior in terms of a superparamagnetic transition is also supported by SQUID measurements of $M_R(T)$ of superparamagnetic epitaxial ultrathin magnetic (Fe_3O_4) films by Voogt *et al.*[76] These authors observed a nearly linear increase of M_R with decreasing T below the blocking temperature, similar to our observation in Fig. 9(b). This rise of M_R with decreasing T is governed by the relaxation time τ, i.e., the time to reverse the magnetic domain (or cluster) magnetization over an energy barrier of height W.[76] An approximately linear increase of the measured magnetization upon cooling below T_B was reported also by Chien[77] and Xiao *et al.*[78] in their work on Fe-(SiO_2) granular films. Thus, there is convincing evidence for a quasilinear T dependence of M_R below T_B in various superpara-

magnetic systems. As the ^{57}Fe hyperfine magnetic field B_{hf} is proportional to the spontaneous magnetization[79] (or to the remanent magnetization in a single magnetic domain), we can expect a quasi-linear B_{hf} versus T behavior below T_B, as experimentally observed in our Fig. 9(b) for ^{57}Fe nanoclusters on GaAs(001). The superparamagnetic behavior in Fe/GaAs(001)-(4×6) at low coverages, i.e., below the critical thickness $d_C \approx 4$ ML Fe at which ferromagnetism occurs, was also inferred from *in situ* Brillouin light scattering by Steinmüller *et al.*[45]

The superparamagnetic relaxation of the magnetization in noninteracting single-domain particles in the zero applied field can be described by the Arrhenius law for the relaxation time τ,[73,77,80]

$$\tau = \tau_0 e^{CV/k_B T}, \tag{2}$$

where k_B is the Boltzmann constant, τ_0^{-1} is the attempt frequency ($\sim 10^{11}$ s^{-1}), C is the magnetic anisotropy constant, V is the cluster volume, T is the temperature, and $CV=W$ is the magnetic anisotropy energy. The observed T_B depends on the characteristic time window of the measurement technique, τ_m. For $\tau \ll \tau_m$, the system behaves superparamagnetically, and for $\tau \gg \tau_m$, the system is in the blocked (frozen) state. T_B is then defined by $\tau = \tau_m$. From

$$T_B = \frac{CV}{k_B[\ln(\tau_m/\tau_0)]}, \tag{3}$$

one can determine the magnetic anisotropy energy (CV) of the clusters using the characteristic Mössbauer observation time $\tau_m \approx 10^{-8}$ s (^{57}Fe nuclear Larmor precession time), the measured T_B values, and choosing $\tau_0 \approx 10^{-11}$ s.[76]

By using our measured T_B values of 62, 80, and 165 K for 1.9, 2.2, and 2.5 ML Fe coverage, respectively, the following values for the anisotropy energy (CV) are obtained: 5.9×10^{-14} erg (37 meV) for 1.9 ML, 7.6×10^{-14} erg (48 meV) for 2.2 ML, and 15.7×10^{-14} erg (98 meV) for 2.5 ML ^{57}Fe coverage. These values, obtained from our ^{57}Fe/GaAs nanoclusters, are of the same order of magnitude as the anisotropy energy obtained by Chien[77] and Xiao *et al.*[78] on $Fe_{50}(SiO_2)_{50}$ nanoparticles of 2.5 nm average diameter, i.e., $CV \approx 8.2\times10^{-14}$ erg.

The average volume V of the ^{57}Fe nanoclusters in our samples has been obtained from our STM results (Sec. III A 2). The average values obtained by STM are 1.84, 20.03, 25.20, and 30.47 nm^3 for Fe coverages of 1, 2.5, 3, and 4 ML, respectively [Fig. 2(e)]. By interpolation, we obtain a cluster volume of 11–12.75 nm^3 at 1.9 ML coverage and 15–16.5 nm^3 at 2.2 ML coverage. This allows us to calculate the magnetic anisotropy constant C in our samples. The C values derived are $(4.6–5.4)\times10^5$ J/m^3 for our 1.9–2.2 ML Fe samples and 7.8×10^5 J/m^3 for our 2.5 ML Fe sample.

4. Discussion of magnetic anisotropy and blocking temperature

Our C values should be compared with literature values of the effective uniaxial magnetic anisotropy constant $K_U^{eff} = K_U^V + K_U^{int}/t_{Fe}$ for Ga-terminated Fe/GaAs(001), as in our case. Here, K_U^V is the volume contribution and K_U^{int} is the interface term that dominates for $t_{Fe} < 10$ ML.[27] Therefore, we may compare our C values with the effective uniaxial anisotropy $K_U^{eff} \approx K_U^{int}/t_{Fe}$ reported in the literature. For the Ga-terminated case, Herfort *et al.*[48] performed SQUID magnetometry on Al-coated samples and obtained $K_U^{eff} = 0.87\times10^5$ J/m^3 at RT for $t_{Fe}=5$ ML. At low temperature ($T=10$ K), Herfort *et al.*[48] obtained $K_U^{eff} = 2.2\times10^5$ J/m^3 for $t_{Fe}=4$ ML, $K_U^{eff} = 0.5\times10^5$ J/m^3 for $t_{Fe}=3$ ML, and $K_U^{eff} \approx 0$ for $t_{Fe}=2.5$ ML. Apparently, K_U^{eff} decreases to about zero (at 2.5 ML) with decreasing Fe coverage. This is surprising since K_U^{eff} is dominated by the interface term K_U^{int}/t_{Fe}, which should increase with decreasing t_{Fe}. The authors[48] regarded this strong reduction of K_U^{eff} below $t_{Fe}=4$ ML (which is accompanied by a strong reduction of the saturation magnetization M_S) as an indication that the structural configuration of the Fe/GaAs interface is not entirely established before the complete coalescence of the Fe islands occurs. Our observation of superparamagnetism for *uncoated* Fe/GaAs(001) at 2.5 ML coverage, together with the high magnetic anisotropy value C of $\sim 7.8\times10^5$ J/m^3 obtained for this film, is in disagreement with the result of Herfort *et al.* on Al-coated Fe/GaAs. We attribute this discrepancy to intermixing and Fe-Al interfacial alloy formation in the Al-coated ultrathin Fe/GaAs films used in Ref. 48 since the formation of interfacial Fe-Al solid solutions and intermetallic compounds has been clearly observed in room-temperature deposited Fe/Al multilayers.[81,82] Fe-Al interface alloying will result in a strong reduction of M_S and K_U^{int} (and K_U^{eff}), particularly at ultrathin Fe coverages of $t_{Fe} \leqslant 2.5$ ML, where our uncoated (free) Fe clusters still show magnetic ordering and large anisotropy at low T.

Moosbühler *et al.*[33] have employed *ex situ* MOKE to determine K_U^{eff} for *Au-coated* epitaxial Fe films on Ga-terminated (4×2) and (2×6) GaAs(001) surfaces as a function of Fe coverage at RT. According to Fig. 4 of Ref. 33, $K_U^{eff} \approx 12\times10^5$ erg/cm^3 ($\approx 1.2\times10^5$ J/m^3) at $t_{Fe}=5$ ML and drops to $K_U^{eff} \approx 10\times10^5$ erg/cm^3 ($\approx 1\times10^5$ J/m^3) at $t_{Fe}=4$ ML for both types of surface reconstructions. These K_U^{eff} values, measured at RT, are smaller than our C values [$C \approx (4.6–5.4)\times10^5$ J/m^3 for $t_{Fe}=1.9-2.2$ ML and $C \approx 7.8\times10^5$ J/m^3 for $t_{Fe}=2.5$ ML] obtained by Mössbauer spectroscopy at low temperatures and at lower Fe coverages, but are of the same order of magnitude. Since magnetic anisotropies usually increase by reducing T, enhanced K_U^{eff} values are expected at lower temperatures. Moreover, K_u^{eff} is expected to increase at lower Fe coverages because of the interface term K_U^{int}/t_{Fe}. Surprisingly, this expected behavior was not observed in the low-temperature magnetometric measurements on Au-coated Fe/GaAs(001) by Bensch *et al.*:[34] At 10 K, $K_U^{int} = K_U^{eff} \cdot t_{Fe}$ was found to drop from ≈ 0.04 erg/cm^2 (or $K_U^{eff} \approx 0.90\times10^5$ J/m^3) at $t_{Fe}=3.1$ ML to zero ($K_U^{eff} \approx 0$) at $t_{Fe}=2.5$ ML. The disappearance of K_U^{eff} at and below $t_{Fe}=2.5$ ML for Au-coated Ga-terminated Fe/GaAs(001) at low T, as observed by Bensch *et al.*,[34] agrees with the low-T result reported by Herfort *et al.*[48] for Al-coated Fe/GaAs(001) samples. However, both results are in striking contrast to our Mössbauer results, which clearly demonstrate, via the appearance of the hyperfine magnetic field $\langle B_{hf} \rangle$ at low T, that uncoated (free) Fe clusters on Ga-

terminated GaAs(001) surfaces at Fe coverages $t_{Fe} \leq 2.5$ ML are intrinsically magnetically ordered and behave superparamagnetically above T_B, implying a large effective anisotropy constant C (or K_U^{eff}). Moreover, our results on uncoated Fe/GaAs films unambiguously demonstrate that contrary to the case of Al-coated[48] and Au-coated[32–34] films, the intrinsic ferromagnetic order within the uncoated Fe clusters does not break down at and below 2.5 ML Fe coverage; this is clearly proven by the persistence of the hyperfine magnetic field $\langle B_{hf} \rangle$ at low T for $t_{Fe} \leq 2.5$ ML in uncoated films. We attribute the discrepancy between the results by Bensch *et al.*[34] and our findings to the influence of the Au coating layer used in Ref. 34. In fact, for the growth of Au on Fe(001) at low temperature (370 K), a surface Au-Fe alloy was observed by STM at submonolayer Au coverage.[83,84] This surface-confined alloy demixes when it is further covered with Au, and in combination with layer-by-layer growth, a rough interface consisting of Au islands and Fe islands on the original Fe(001) substrate is created.[83,84] Apparently, such a severe Au-Fe surface alloying affects the magnetic properties of ultrathin Fe layers (saturation magnetization M_S and uniaxial interface magnetic anisotropy K_U^{int}), particularly at very low Fe coverages, such as $t_{Fe} \leq 2.5$ ML, and leads to $M_S \approx 0$ and $K_U^{int} \approx 0$ at low temperatures ($T \rightarrow 0$ K). By contrast, our uncoated free Fe nanoclusters on GaAs manifest the real intrinsic properties of this system, unaffected by surface-coating materials.

The only literature report on uncoated (free) Fe/GaAs(001)-(4×6) ultrathin films in UHV at low temperature is that of Zakeri *et al.*[53] These researchers performed *in situ* ferromagnetic resonance (FMR) studies in UHV in the temperature range of 40 K $\leq T \leq$ 400 K at Fe coverages between 5–20 ML. Due to experimental limitations, they could measure only the perpendicular component of the anisotropy constant. They reported a strong *perpendicular* surface anisotropy contribution of $K_{2\perp}^{s,eff} = 1.26 \times 10^{-3}$ J/m^2 and a smaller volume contribution of $K_{2\perp}^{v} = (4 \pm 9) \times 10^4$ J/m^3 (both values obtained from extrapolation to $T=0$ K). For the thinnest Fe coverage ($t_{Fe}=5$ ML) at 40 K, one can estimate a value of $K_{2\perp}^{eff} \approx 16 \times 10^5$ J/m^3 from the insert in Fig. 4 of Ref. 53. This value, obtained by FMR at low T, is of the same order of magnitude as our anisotropy values of $C \approx 5 \times 10^5$ J/m^3 (at $t_{Fe}=1.9$–2.2 ML) and $C \approx 7.8 \times 10^5$ J/m^3 (at $t_{Fe}=2.5$ ML), also determined on uncoated (free) Fe/GaAs(001)-(4×6) in UHV at low temperatures. The appearance of an out-of-plane anisotropy component agrees with theoretical predictions by Košuth *et al.*[85] who found that a part of the magnetic anisotropy energy favors an out-of-plane orientation for GaAs(001)/Fe$_n$ ($n=1$–7 ML).

Moreover, large effective perpendicular (out-of-plane) surface/interface anisotropy constants were observed at RT by McPhail *et al.*[42] on Au-coated 4.1 ML thick Fe/GaAs(001)-(4×6) by *ex situ* polar MOKE measurements ($|K_p^{eff}| = 15 \times 10^5$ J/m^3) and by Madami *et al.*[47] on uncoated 5 Å thick (3.5 ML) Fe/GaAs(001)-(4×6) by *in situ* Brillouin light scattering ($K_{out}^{eff} = K_{out}^{s}/t_{Fe} = 8.0 \times 10^5$ J/m^3). Some of the measured $K_{2\perp}^{eff} = K_{out}^{eff}$ values are larger than the demagnetization energy $2\pi M_S^2 = 16.1 \times 10^5$ J/m^3 of Fe, forcing the magnetization in the film plane. However, the strong uniaxial in-plane surface anisotropy has to be subtracted from these $K_{2\perp}^{eff}$ values, reducing them to values below $2\pi M_S^2$ and leaving the magnetization in the film plane. These values are of the same order of magnitude as our C values. It is interesting in this context that strong effective perpendicular anisotropy constants $K_{2\perp}$ of 14.6×10^5 J/m^3 at $t_{Fe}=4$ ML and 2.1×10^5 J/m^3 at $t_{Fe}=33$ ML were also determined by ferromagnetic resonance for the case of epitaxial Fe layers on GaAs(001) surfaces that were As capped (and As desorbed in UHV) before Fe deposition.[44] This desorption of the As cap layer usually leads to an As-terminated GaAs(001) surface,[52] but the magnetic anisotropy is known to be fairly independent of the GaAs(001) surface reconstruction.[33,48] These large $K_{2\perp}$ values[44] are in qualitative agreement with our anisotropy (C) values obtained by Mössbauer spectroscopy. However, since Zhai *et al.*[44] gave neither their measurement temperature nor the type of protective coating material, we cannot draw further conclusions from this comparison.

We now compare our superparamagnetic blocking temperatures T_B (measured in zero-external field *in situ* in UHV on uncoated Fe films) with magnetic transition temperatures for Fe/GaAs(001) reported in the literature. Unfortunately, with one exception, we can compare only with Au-coated or Al-coated Fe films reported in the literature. Bensch *et al.*[32] measured the Fe-thickness dependence of the transition temperatures T_C by *ex situ* MOKE on Au-coated wedge-shaped Fe films at Fe coverages between $2.8 \leq t_{Fe} \leq 3.6$ ML. They interpreted their T_C as the magnetic ordering temperature of a 2D system and could describe T_C vs t_{Fe} by a finite-size scaling law, which (extrapolated to $T_C=0$ K) resulted in a critical thickness of $t_{Fe}=2.5$ ML for the onset of ferromagnetism.[32] However, the lowest measurement temperature in Ref. 32 was only about 100 K. Keeping Eq. (3) in mind, we can predict from our superparamagnetic blocking temperature T_B (Möss) (measured by CEMS) the blocking temperature T_B (MOKE/SQUID) expected from a magnetometric MOKE (and SQUID) measurement on the same sample by using the ratio defined in Ref. 77,

$$\frac{T_B(\text{MOKE/SQUID})}{T_B(\text{Möss})} = \frac{\ln(\tau_2/\tau_0)}{\ln(\tau_1/\tau_0)}. \tag{4}$$

Here, $\tau_1 \approx 10$–100 s is the characterization observation time in MOKE (and SQUID) measurements,[76,77] and $\tau_2 = \tau_m \approx 10^{-8}$ in a Mössbauer measurement. For an ac-MOKE measurement (as performed by Bensch *et al.*[32]), $\tau_1 \approx 10^{-2}$ s. The predicted values of T_B (MOKE/SQUID) range from 14–22, 18–28, and 38–58 K for our samples with $t_{Fe}=1.9$, 2.2, and 2.5 ML, respectively. In the case of ac-MOKE, the predicted values are about 20, 26, and 54 K for analogous Fe thicknesses. None of these temperatures were accessible in the work by Bensch *et al.*[32] Ploog *et al.*[40] mentioned a T_B value of 30 K at 2.5 ML Fe in their work; however, below 2.5 ML, these researchers did not observe a magnetic signal, contrary to what is obtained from our Mössbauer results on uncoated Fe/GaAs films. This discrepancy may be explained by Fe-Al intermixing due to the Al coating layer used in that work.

Similarly, in the low-temperature SQUID work by Bensch *et al.*[34] no magnetic signal was detected at 10 K for $t_{Fe} \leq 2.5$ ML, very likely due to Fe-Au intermixing with the Au coating layer. By contrast, Zakeri *et al.*[86] reported a superparamagnetic blocking temperature of 50 K at approximately 2.3 ML Fe coverage in their recent *in situ* FMR study on uncoated Fe/GaAs(001). This value is in fair agreement with our T_B values of ~60–80 K, also obtained on uncoated Fe films of similar coverages.

C. Lattice dynamics

For an isotropic system with lattice vibrations in the harmonic approximation, the recoil-energy free fraction f of the nuclear resonant absorption events at temperature T (the Debye-Waller factor or Lamb-Mössbauer factor, or simply f factor) is given by Ref. 71: $f(T)=\exp(-k^2\langle x^2\rangle)$, where $\langle x^2\rangle$ is the mean-square displacement of the ^{57}Fe nucleus along the γ-ray direction and k is the wave vector of the γ radiation. In the Debye model, f is expressed by[87]

$$f(T) = \exp\left\{ -\left[\frac{3E_R}{2k_B\Theta_D} \right]\left[1 + 4\left(\frac{T}{\Theta_D} \right)^2 \int_0^{\Theta/T} \frac{x}{\exp x - 1} dx \right] \right\}. \quad (5)$$

Here, k_B is the Boltzmann constant, Θ_D is the Debye temperature, the integral is known as the Debye integral, and E_R is the recoil energy of the free ^{57}Fe nucleus ($E_R=1.956\,275 \times 10^{-3}$ eV for ^{57}Fe).

The f factor is known to be proportional to the normalized spectral area A of the Mössbauer spectrum (normalized by the nonresonant number of counts).[88] In Fig. 9(c), we have plotted the T dependence of the reduced spectral area $A(T)/A_{av}$ of our three samples, obtained from the CEM spectra in Figs. 6–8. (A_{av} is the average reduced spectral area, averaged over the low-T values between 27 and 40 K). The T dependence of the reduced spectral area was calculated from Eq. (5) and least-squares fit to the experimental spectral area ratio of ^{57}Fe/GaAs(001) with 2.2 ML Fe coverage [full circles in Fig. 9(c)]. From this fitting [full-drawn curve in Fig. 9(c)], we obtain a Debye temperature Θ_D of 196±4 K for the Fe nanoclusters at 2.2 ML coverage. As can be noticed in Fig. 9(c), the experimental data points for 1.9 ML Fe coverage [Fig. 9(c), triangles] are also, on the average, well described by the fit curve for $\Theta_D=196$ K. On the other hand, above ~100 K, the data points for the sample with 2.5 ML Fe coverage [Fig. 9(c), full squares] are systematically higher than the fit curve, implying a somewhat larger Debye temperature than 196 K for this sample. The value of $\Theta_D=196$ K for the Fe nanoclusters is strikingly smaller than the Debye temperature of 433±8 K for bulk bcc-Fe.[89]

The softening of the lattice vibrations revealed by the drastic reduction of Θ_D in our Fe nanoclusters on GaAs(001) can be caused by two (probably superimposed) effects: (i) interfacial Fe-Ga and/or (less likely) Fe-As alloy formation and (ii) modification of the phonon density of states, $g(E)$, due to the finite size of the Fe nanoclusters. In fact, a shift of $g(E)$ to lower phonon energies has been observed experimentally in nanocrystalline Fe (Ref. 90) and has been predicted theoretically for metallic nanoclusters,[91–93] which leads to a reduction of f and Θ_D. Further, $g(E)$ at the interface between the continuous Fe film and a semiconductor similar to GaAs(001), namely, InAs(001), has been measured by nuclear resonant inelastic x-ray scattering and found to be drastically enhanced at low phonon energies[94] as compared to that of bulk bcc-Fe, resulting in strongly reduced values of f and Θ_D. The strong phonon softening in the Fe nanoclusters observed here and in other systems[95] will have implications for phonon-related and phonon-assisted phenomena in this system (such as thermodynamical properties, preexponential factors, e.g., in surface diffusion, and $1/f$ electronic noise).

IV. CONCLUSIONS

The growth, structure, hyperfine magnetic properties, and lattice vibrational dynamics of uncoated bcc-^{57}Fe(001) ultrathin films deposited at ~50 °C onto GaAs(001)-(4×6) surfaces have been investigated *in situ* in UHV by STM, LEED/RHEED, XPS, and ^{57}Fe CEMS. Up to 3.6 ML Fe coverage, RHEED images still display reflections from the GaAs(001) substrate, demonstrating incomplete coalescence of Fe islands (nanoclusters). This is corroborated in real space by STM, where for $t_{Fe}=1$ ML coverage, small Fe clusters with heights of 1–2 ML are arranged in rows along the [110] direction. Upon increase of the Fe coverage to 2.5 ML, the Fe cluster size-distribution becomes more homogeneous, and the clusters appear to be mostly 2 ML high and are connected along the [−110], but not along the [110] direction, suggesting that the onset of ferromagnetism at RT would not arise at $t_{Fe}=2.5$ ML. Upon increasing the Fe coverage to $t_{Fe}=3$ ML, the surface morphology consists of percolated Fe clusters without preferential orientation, and deposition of 4 ML Fe leads to a fairly smooth surface with the same surface roughness of 2 ML in height. The effect of intermixing between the Fe overlayers and repelled Ga and As atoms from the substrate was investigated by XPS. The deposition of 1 ML Fe leads to a moderate increase of the Ga and As 3d binding energies, indicating a substantial change in the Ga and As coordination and, predominantly, Fe-GaAs interactions as the origin of the moderate shift in the binding energy. At $t_{Fe}=2.5$ ML, only slight shifts of the binding energy of Ga 3d and As 3d levels are observed, which is attributed to an increase of the Fe-Fe coordination. At larger coverages (4 ML Fe), segregation of Ga atoms appears to occur since an additional XPS satellite is observed below a binding energy of 18 eV. This shoulder is attributed to repelled Ga atoms diffusing to the surface of the Fe layer.

Epitaxial bcc-^{57}Fe ultrathin films at Fe coverages of 1.9, 2.2, and 2.5 ML on GaAs(001)-(4×6) surfaces were investigated *in situ* in UHV by ^{57}Fe CEMS in zero-external field in the temperature range between 27 K and room temperature. At such low coverages, these uncoated (free) Fe films consist predominantly of isolated Fe nanoclusters below their percolation threshold. At the lowest temperatures (27–40 K), we find magnetic ordering for all samples, as evidenced by the appearance of a large mean hyperfine magnetic field $\langle B_{hf}\rangle$ of ~22–23 T. This value is about the same

for all Fe coverages investigated, demonstrating that the hyperfine field near a magnetic saturation (extrapolated to $T=0$ K) is nearly independent of the Fe cluster size and is an intrinsic property of the magnetically ordered clusters. The observed approximately quasilinear decrease of $\langle B_{hf} \rangle$ with T is typical for superparamagnetic systems and provides superparamagnetic blocking temperatures T_B of 62 ± 5, 80 ± 10, and 165 ± 5 K for $t_{\mathrm{Fe}}=1.9$, 2.2, and 2.5 ML, respectively. Our present results demonstrate that the nature of the percolation transition for free (uncoated) Fe nanoclusters on GaAs(001) in UHV is from superparamagnetism to ferromagnetism and not from paramagnetism to ferromagnetism. The magnetic anisotropy energies CV for the superparamagnetic relaxation are estimated to be 37, 48, and 98 meV for 1.9, 2.2, and 2.5 ML Fe, respectively. Combined with the average Fe nanoparticle volume, determined by STM, this leads to a large magnetic anisotropy constant C of $\sim 5\times10^5$ J/m^3 for 1.9–2.2 ML Fe and of $\sim 8\times10^5$ J/m^3 at 2.5 ML Fe. Our values are of the same order of magnitude as the out-of-plane magnetic anisotropy components obtained by *in situ* FMR on uncoated Fe/GaAs(001) at 40 K and 5 ML coverage[53] and by *in situ* Brillouin light scattering on uncoated Fe/GaAs(001) at RT.[47] However, our findings are at variance with those of other groups,[34,48] who have investigated *metal-coated* ultrathin Fe films on GaAs(001) at low temperatures and who do not observe magnetic ordering at coverages $t_{\mathrm{Fe}} \leqslant 2.5$ ML. This discrepancy emphasizes the importance of *in situ* experiments in UHV on uncoated Fe clusters in order to probe their intrinsic magnetic properties. From the T dependence of the Mössbauer spectral area, a strikingly low Debye temperature Θ_D of (196 ± 4) K is deduced for uncoated Fe nanoclusters on GaAs(001) at 1.9–2.2 ML coverage in UHV, indicating strong phonon softening and severe modifications of the phonon density of states in the clusters as compared to bulk bcc-Fe. This has a strong impact on the thermodynamic properties of these clusters.

ACKNOWLEDGMENTS

We are very grateful to Ulrich von Hörsten for his expert technical assistance and Marco Walterfang for helpful discussions. This work was financially supported by Deutsche Forschungsgemeinschaft (GK 277 and SFB 491), National Science Foundation under Grant No. 044849, and ACS-Petroleum Research Foundation (ACS-PRF Award No. 42701-G5).

*Author to whom correspondence should be addressed. roldan@physics.ucf.edu

†Permanent address: Tohoku University, Sendai, Japan.

[1] G. Wastlbauer and J. A. C. Bland, Adv. Phys. **54**, 137 (2005), and references therein before the year 2005.

[2] G. A. Prinz, Science **250**, 1092 (1990).

[3] S. A. Wolf, D. D. Awschalom, R. A. Buhrman, J. M. Daughton, and S. von Molnar, Science **294**, 1488 (2001).

[4] I. Zutic, J. Fabian, and S. Das Sarma, Rev. Mod. Phys. **76**, 323 (2004).

[5] B. T. Jonker, A. T. Hanbicki, Y. D. Park, G. Itskos, M. Furis, G. Kioseoglău, A. Petrou, and X. Wei, Appl. Phys. Lett. **79**, 3098 (2001).

[6] H. J. Zhu, M. Ramsteiner, H. Kostial, M. Wassermeier, H.-P. Schönherr, and K. H. Ploog, Phys. Rev. Lett. **87**, 016601 (2001).

[7] A. T. Hanbicki, O. M. J. van't Erve, R. Magno, G. Kioseoglău, C. H. Li, B. T. Jonker, G. Itskos, R. Mallory, M. Yasar, and A. Petrou, Appl. Phys. Lett. **82**, 4092 (2003).

[8] O. M. J. van't Erve, G. Kioseoglău, A. T. Hanbicki, C. H. Li, B. T. Jonker, R. Mallory, M. Yasar, and A. Petrou, Appl. Phys. Lett. **84**, 4334 (2004).

[9] N. C. Gerhardt, S. Hövel, C. Brenner, M. R. Hofmann, F.-Y. Lo, D. Reuter, A. D. Wieck, E. Schuster, W. Keune, and K. Westerholt, Appl. Phys. Lett. **87**, 032502 (2005).

[10] C. Adelmann, X. Lou, J. Strand, C. J. Palmstrom, and P. A. Crowell, Phys. Rev. B **71**, 121301(R) (2005).

[11] A. T. Hanbicki, B. T. Jonker, G. Itskos, G. Kioseoglou, and A. Petrou, Appl. Phys. Lett. **80**, 1240 (2002).

[12] A. Hirohata, Y. B. Xu, C. M. Guertler, J. A. C. Bland, and S. N. Holmes, Phys. Rev. B **63**, 104425 (2001).

[13] J. R. Waldrop and R. W. Grant, Appl. Phys. Lett. **34**, 630 (1979).

[14] G. A. Prinz and J. J. Krebs, Appl. Phys. Lett. **39**, 397 (1981).

[15] J. J. Krebs, B. T. Jonker, and G. A. Prinz, J. Appl. Phys. **61**, 2596 (1987).

[16] J. M. Florczak and E. D. Dahlberg, Phys. Rev. B **44**, 9338 (1991).

[17] C. Daboo, R. J. Hicken, E. Gu, M. Gester, S. J. Gray, D. E. P. Eley, E. Ahmad, J. A. C. Bland, R. Ploessl, and J. N. Chapman, Phys. Rev. B **51**, 15964 (1995).

[18] M. Gester, C. Daboo, R. J. Hicken, S. J. Gray, A. Ercole, and J. A. C. Bland, J. Appl. Phys. **80**, 347 (1996).

[19] P. M. Thibado, E. Kneedler, B. T. Jonker, B. R. Bennett, B. V. Shanabrook, and L. J. Whitman, Phys. Rev. B **53**, R10481 (1996).

[20] E. Kneedler, P. M. Thibado, B. T. Jonker, B. R. Bennett, B. V. Shanabrook, R. J. Wagner, and L. J. Whitman, J. Vac. Sci. Technol. B **14**, 3193 (1996).

[21] E. M. Kneedler, B. T. Jonker, P. M. Thibado, R. J. Wagner, B. V. Shanabrook, and L. J. Whitman, Phys. Rev. B **56**, 8163 (1997).

[22] E. M. Kneedler and B. T. Jonker, J. Appl. Phys. **81**, 4463 (1997).

[23] Y. B. Xu, E. T. M. Kernohan, D. J. Freeland, A. Ercole, M. Tselepi, and J. A. C. Bland, Phys. Rev. B **58**, 890 (1998).

[24] Y. B. Xu, E. T. M. Kernohan, D. J. Freeland, M. Tselepi, A. Ercole, and J. A. C. Bland, J. Magn. Magn. Mater. **198-199**, 703 (1999).

[25] D. J. Freeland, Y. B. Xu, E. T. M. Kernohan, M. Tselepi, and J. A. C. Bland, Thin Solid Films **343-344**, 210 (1999).

[26] M. Zölfl, M. Brockmann, M. Köhler, S. Kreuzer, T. Schweinböck, S. Miethaner, F. Bensch, and G. Bayreuther, J. Magn. Magn. Mater. **175**, 16 (1997).

[27] M. Brockmann, M. Zölfl, S. Miethaner, and G. Bayreuther, J. Magn. Magn. Mater. **198-199**, 384 (1999).

[28] A. Filipe, A. Schuhl, and P. Galtier, Appl. Phys. Lett. **70**, 129 (1997).

[29] A. Filipe and A. Schuhl, J. Appl. Phys. **81**, 4359 (1997).
[30] B. Lépine, S. Ababou, A. Guivarc'h, G. Jezequel, S. Deputier, R. Guerin, A. Filipe, A. Schuhl, F. Abel, C. Cohen, A. Rocher, and J. J. Crestou, J. Appl. Phys. **83**, 3077 (1998).
[31] R. A. Gordon, E. D. Crozier, D.-T. Jiang, T. L. Monchesky, and B. Heinrich, Phys. Rev. B **62**, 2151 (2000).
[32] F. Bensch, G. Garreau, R. Moosbühler, G. Bayreuther, and E. Beaurepaire, J. Appl. Phys. **89**, 7133 (2001).
[33] R. Moosbühler, F. Bensch, M. Dumm, and G. Bayreuther, J. Appl. Phys. **91**, 8757 (2002).
[34] F. Bensch, R. Moosbühler, and G. Bayreuther, J. Appl. Phys. **91**, 8754 (2002).
[35] M. Doi, B. Roldan Cuenya, W. Keune, T. Schmitte, A. Nefedov, H. Zabel, D. Spoddig, R. Meckenstock, and J. Pelzl, J. Magn. Magn. Mater. **240**, 407 (2002).
[36] J. W. Freeland, I. Coulthard, W. J. Antel, Jr., and A. P. J. Stampfl, Phys. Rev. B **63**, 193301 (2001).
[37] Y. Chye, V. Huard, M. E. White, and P. M. Petroff, Appl. Phys. Lett. **80**, 449 (2002).
[38] S. J. Steinmüller, M. Tselepi, V. Strom, and J. A. C. Bland, J. Appl. Phys. **91**, 8679 (2002).
[39] H. P. Schönherr, R. Nötzel, W. Ma, and K. H. Ploog, J. Appl. Phys. **89**, 169 (2001).
[40] K. H. Ploog, J. Herfort, H.-P. Schönherr, M. Moreno, and S. Dhar, J. Cryst. Growth **251**, 292 (2003).
[41] B. Roldan Cuenya, M. Doi, W. Keune, S. Hoch, D. Reuter, A. Wieck, T. Schmitte, and H. Zabel, Appl. Phys. Lett. **82**, 1072 (2003).
[42] S. McPhail, C. M. Gürtler, F. Montaigne, Y. B. Xu, M. Tselepi, and J. A. C. Bland, Phys. Rev. B **67**, 024409 (2003).
[43] O. Thomas, Q. Shen, P. Schieffer, N. Tournerie, and B. Lepine, Phys. Rev. Lett. **90**, 017205 (2003).
[44] Y. Zhai, L. Shi, W. Zhang, Y. X. Xu, M. Lu, H. R. Zhai, W. X. Tang, X. F. Jin, Y. B. Xu, and J. A. C. Bland, J. Appl. Phys. **93**, 7622 (2003).
[45] S. J. Steinmüller, M. Tselepi, G. Wastlbauer, V. Strom, D. M. Gillingham, A. Ionescu, and J. A. C. Bland, Phys. Rev. B **70**, 024420 (2004).
[46] J. S. Claydon, Y. B. Xu, M. Tselepi, J. A. C. Bland, and G. van der Laan, Phys. Rev. Lett. **93**, 037206 (2004).
[47] M. Madami, S. Tacchi, G. Carlotti, G. Gubbiotti, and R. L. Stamps, Phys. Rev. B **69**, 144408 (2004).
[48] J. Herfort, W. Braun, A. Trampert, H.-P. Schönherr, and K. H. Ploog, Appl. Surf. Sci. **237**, 181 (2004).
[49] A. Ionescu, M. Tselepi, D. M. Gillingham, G. Wastlauer, S. J. Steinmüller, H. E. Beere, D. A. Ritchie, and J. A. C. Bland, Phys. Rev. B **72**, 125404 (2005).
[50] N. A. Morley, S. L. Tang, M. R. J. Gibbs, E. Ahmad, I. G. Will, and Y. B. Xu, J. Appl. Phys. **97**, 10H501 (2005).
[51] L. Giovanelli, G. Panaccione, G. Rossi, M. Fabrizioli, C.-S. Tian, P. L. Gastelois, J. Fujii, and C. H. Back, Phys. Rev. B **72**, 045221 (2005).
[52] E. Schuster, W. Keune, F.-Y. Lo, D. Reuter, A. Wieck, and K. Westerholt, Superlattices Microstruct. **37**, 313 (2005).
[53] Kh. Zakeri, Th. Kebe, J. Lindner, and M. Farle, Phys. Rev. B **73**, 052405 (2006).
[54] P. Schieffer, A. Guivarc'h, C. Lallaizon, B. Lépine, D. Sébilleau, P. Turban, and G. Jézéquel, Appl. Phys. Lett. **89**, 161923 (2006).
[55] R. A. Gordon and E. D. Crozier, Phys. Rev. B **74**, 165405 (2006).
[56] S. A. Chambers, F. Xu, H. W. Chen, I. M. Vitomirov, S. B. Anderson, and J. H. Weaver, Phys. Rev. B **34**, 6605 (1986).
[57] M. W. Ruckman, J. J. Joyce, and J. H. Weaver, Phys. Rev. B **33**, 7029 (1986).
[58] T. L. Monchesky, R. Urban, B. Heinrich, M. Klaua, and J. Kirschner, J. Appl. Phys. **87**, 5167 (2000).
[59] T. L. Monchesky, A. Enders, R. Urban, K. Myrtle, B. Heinrich, X.-G. Zhang, W. H. Butler, and J. Kirschner, Phys. Rev. B **71**, 214440 (2005).
[60] A. Schatz and W. Keune, Surf. Sci. **440**, L841 (1999).
[61] R. A. Brand, Nucl. Instrum. Methods Phys. Res. B **28**, 417 (1987).
[62] Q.-K. Xue, T. Hashizume, and T. Sakurai, Surf. Sci. **141**, 244 (1999).
[63] J. Behrend, M. Wassermeier, L. Däweritz, and K. H. Ploog, Surf. Sci. **342**, 63 (1995).
[64] D. K. Biegelsen, R. D. Bringans, J. E. Northrup, and L. E. Swartz, Phys. Rev. B **41**, 5701 (1990).
[65] J. F. Moulder, W. F. Stickle, P. E. Sobol, and K. D. Bomben, in *Handbook of X-Ray Photoelectron Spectroscopy*, edited by J. Chastain and R. C. King, Jr. (Physical Electronics, Eden Prairie, MN, 1995).
[66] L. Zhang, R. Persaud, and T. E. Madey, Phys. Rev. B **56**, 10549 (1997).
[67] S. Mirbt, S. Sanyal, C. Isheden, and B. Johansson, Phys. Rev. B **67**, 155421 (2003).
[68] S. C. Erwin, S.-H. Lee, and M. Scheffler, Phys. Rev. B **65**, 205422 (2002).
[69] D. L. Williamson, in *Mössbauer Isomer Shifts*, edited by G. K. Shenoy and F. E. Wagner (North-Holland, Amsterdam, 1978), p. 317.
[70] L. R. Newkirk and C. C. Tsuei, Phys. Rev. B **4**, 4046 (1971).
[71] G. K. Wertheim, *Mössbauer-Effect: Principles and Applications* (Academic, New York, 1964), p. 69.
[72] H. Spies, Diploma thesis, Gerhard-Mercator University, Duisburg, Germany, 2000 (in German).
[73] J. L. Dormann, D. Fiorani, and E. Tronc, Adv. Chem. Phys. **98**, 283 (1997).
[74] It is not clear whether the oscillations in $P(B_{hf})$ observed, in particular, at 40 and 50 K are physically significant or are an artifact of the mathematical fitting procedure; we think that the overall width of $P(B_{hf})$ and the average hf field are not significantly affected by such details of the distribution.
[75] M. F. Thomas and C. E. Johnson, in *Mössbauer Spectroscopy*, edited by D. P. E. Dickson and F. J. Berry (Cambridge University Press, Cambridge, England, 1986), p. 143. See also Fig. 4.29 in this reference.
[76] F. C. Voogt, T. T. M. Palstra, L. Niesen, O. C. Rogojanu, M. A. James, and T. Hibma, Phys. Rev. B **57**, R8107 (1998).
[77] C. L. Chien, J. Appl. Phys. **69**, 5267 (1991).
[78] G. Xiao, S. H. Liou, A. Levy, J. N. Taylor, and C. L. Chien, Phys. Rev. B **34**, 7573 (1986).
[79] R. S. Preston, S. S. Hanna, and J. Heberle, Phys. Rev. **128**, 2207 (1962).
[80] S. Mørup, J. A. Dumesic, and H. Topsøe, in *Applications of Mössbauer Spectroscopy*, edited by R. L. Cohen (Academic, New York, 1980), Vol. II.
[81] M. Carbucicchio, M. Rateo, G. Ruggiero, and G. Turilli, Hyperfine Interact. **113**, 303 (1998).
[82] E. Fonda and A. Traverse, J. Magn. Magn. Mater. **268**, 292

(2004).
[83] M. M. J. Bischoff, T. Yamada, A. J. Quinn, R. G. P. van der Kraan, and H. van Kempen, Phys. Rev. Lett. **87**, 246102 (2001).
[84] M. M. J. Bischoff, T. K. Yamada, and H. van Kempen, Phys. Rev. B **67**, 165403 (2003).
[85] M. Košuth, V. Popescu, H. Ebert, and G. Bayreuther, Europhys. Lett. **72**, 816 (2005).
[86] Kh. Zakeri, Th. Kebe, J. Lindner, and M. Farle, J. Magn. Magn. Mater. **316**, e334 (2007).
[87] G. K. Shenoy, F. E. Wagner, and G. M. Kalvius, in *Mössbauer Isomer Shifts*, edited by G. K. Shenoy and F. E. Wagner (North-Holland, Amsterdam, 1978), p. 49.
[88] D. A. Shirley, M. Kaplan, and P. Axel, Phys. Rev. **123**, 816 (1961).
[89] R. Lübbers, H. F. Grünsteudel, A. I. Chumakov, and G. Wortmann, Science **287**, 1250 (2000).
[90] B. Fultz, C. C. Ahn, E. E. Alp, W. Sturhahn, and T. S. Toellner, Phys. Rev. Lett. **79**, 937 (1997).
[91] A. Kara and T. S. Rahman, Phys. Rev. Lett. **81**, 1453 (1998).
[92] D. Y. Sun, X. G. Gong, and X. Q. Wang, Phys. Rev. B **63**, 193412 (2001).
[93] R. Meyer, L. J. Lewis, S. Prakash, and P. Entel, Phys. Rev. B **68**, 104303 (2003).
[94] R. Peters, E. Schuster, B. Roldan Cuenya, W. Keune, W. Sturhahn, T. S. Toellner, and E. E. Alp (unpublished).
[95] B. Roldan Cuenya, A. Naitabdi, J. Croy, W. Sturhahn, J. Y. Zhao, E. E. Alp, R. Meyer, D. Sudfeld, E. Schuster, and W. Keune (unpublished).